1. Moment-tensor analysis using global data
2. The Harvard (= Global) CMT catalog
3. Using calibration information in waveform analysis
4. Data quality control using noise
5. Data quality control using signals
6. Finding interesting things in the noise

Faulting force model

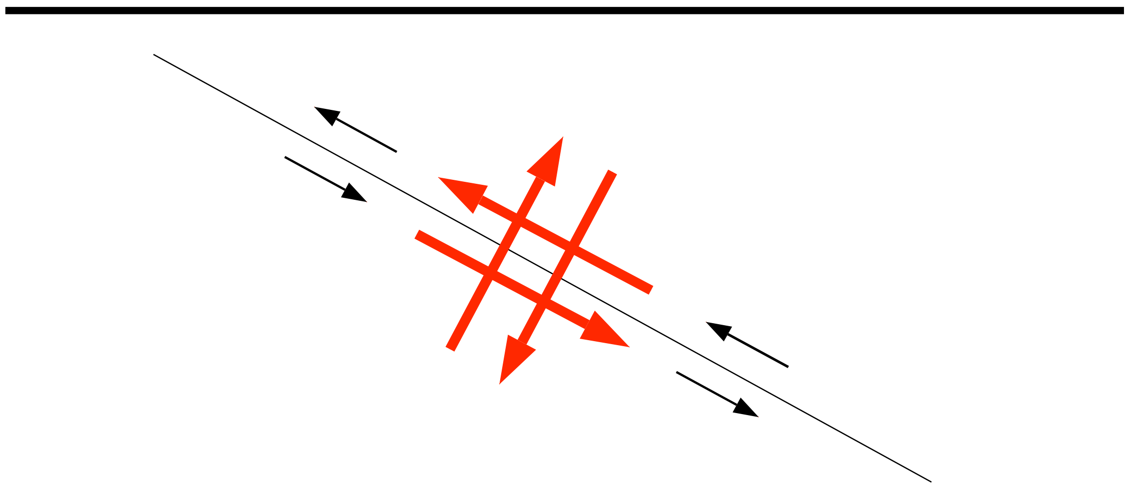

The elastic stress release in an earthquake is described by a double couple of forces

The nine dipoles of the seismic moment tensor

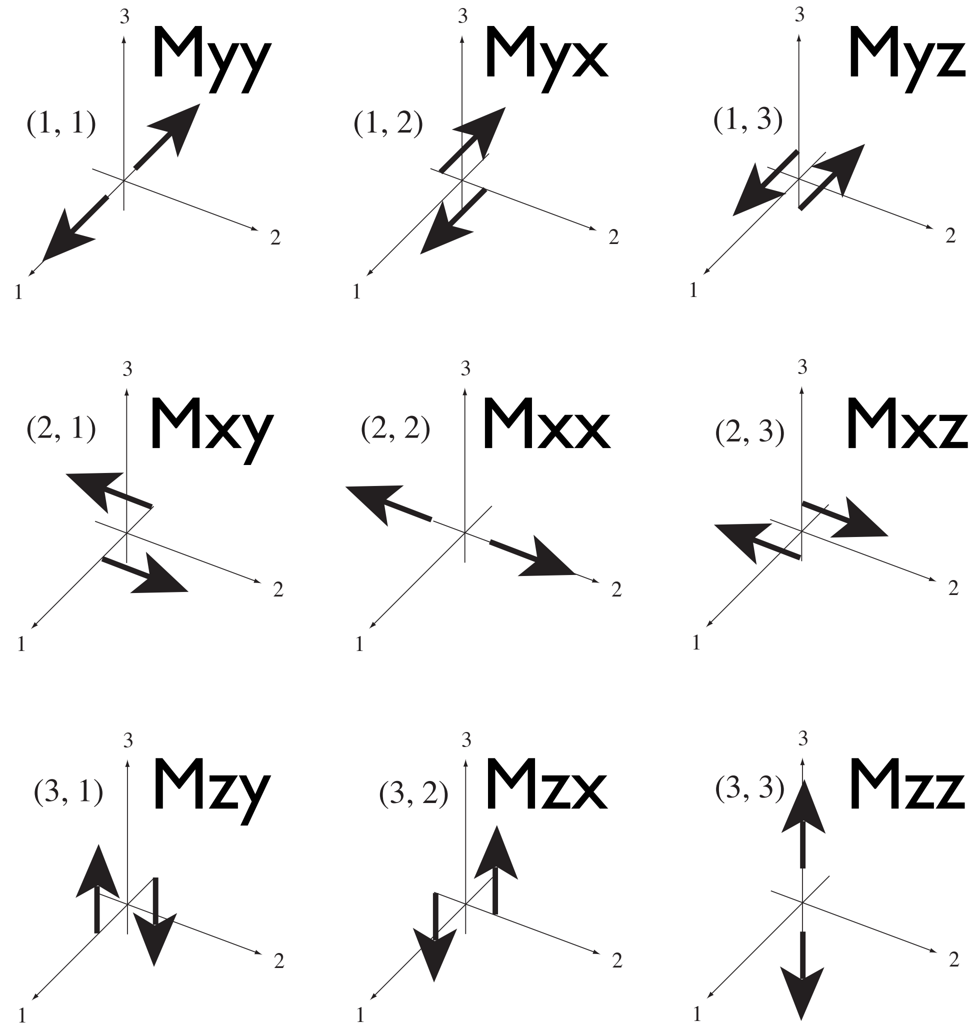

(Aki and Richards, 2002)

But, $M_{xy}=M_{yx}$, $M_{yz}=M_{zy}$, $M_{xz}=M_{zx}$

M_{xy} = 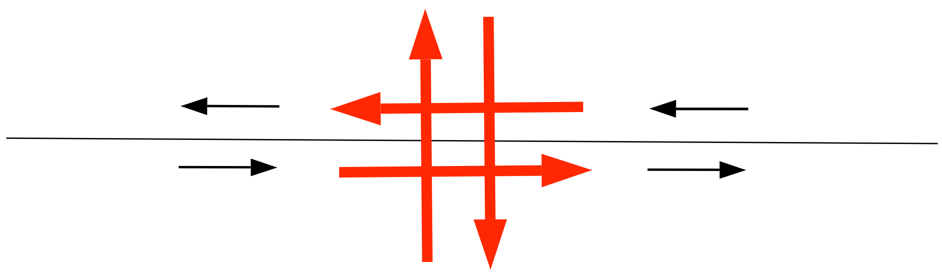 = 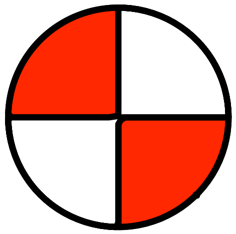

for example,

10^{28} dyne-cm = 10^{24} dyne x 10000 cm

Calculated force seismograms (6000 km distance)

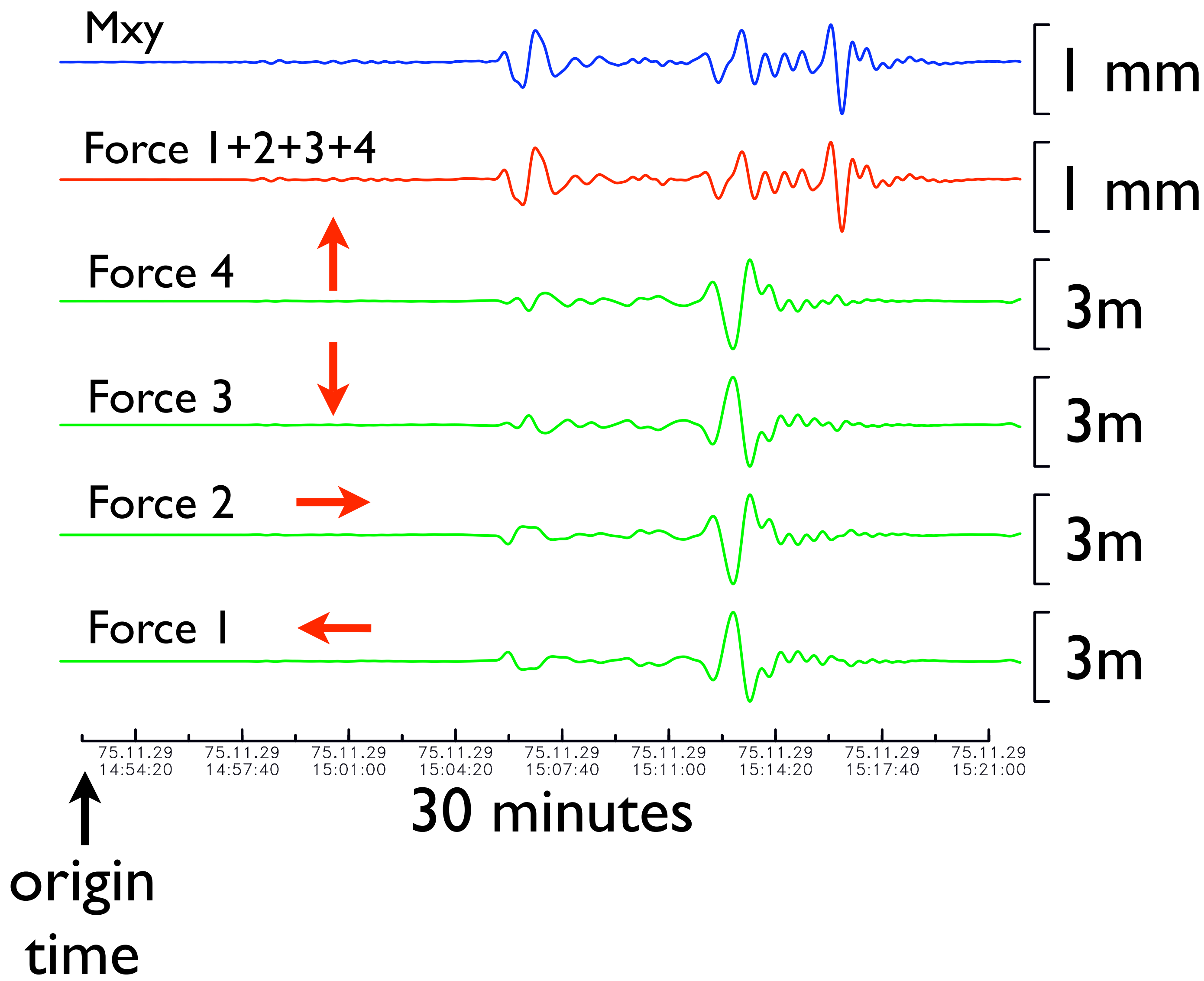

The vibrations caused by a force acting on or in the Earth can be modeled by summation of Earth's normal modes

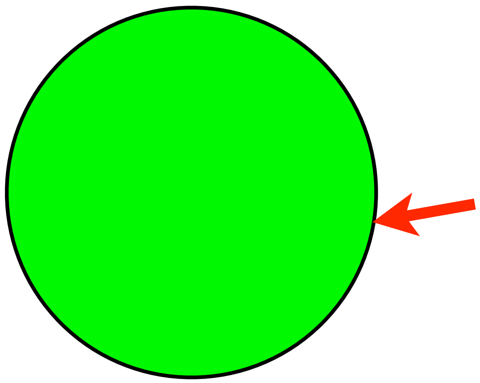

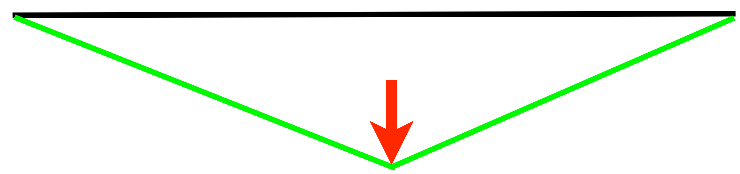

$$u(\boldsymbol{x},t) = \sum_k \left[1 - \exp\left[-\alpha_k(t-t_s)\right] \cos \omega_k(t-t_s)\right] \boldsymbol{f}\cdot\boldsymbol{w}^{(k)}(\boldsymbol{x}_s)\boldsymbol{s}_k(\boldsymbol{x})$$

where $\boldsymbol{f}$ is the force vector and $\boldsymbol{w}^k$ is the displacement of the k-*th* mode.

Moment-tensor analysis by waveform fitting

(Observed seismogram)/(Instrument response) x Filter = Observed waveform

(Synthetic displacement seismogram) x Filter = Model waveform

Model waveform depends on:
1. Earthquake parameters
2. Earth structure

If the Earth structure and the earthquake location are known, the

Model waveform depends only on the six elements of the moment tensor,

M_{xx}, M_{yy}, M_{zz}, M_{xy}, M_{xz}, and M_{yz}

Minimize the difference [Observed waveform - Model waveform]^2

with respect to the moment tensor elements.

Detection and analysis of large earthquakes:

GLOBAL SEISMOGRAPHIC NETWORK

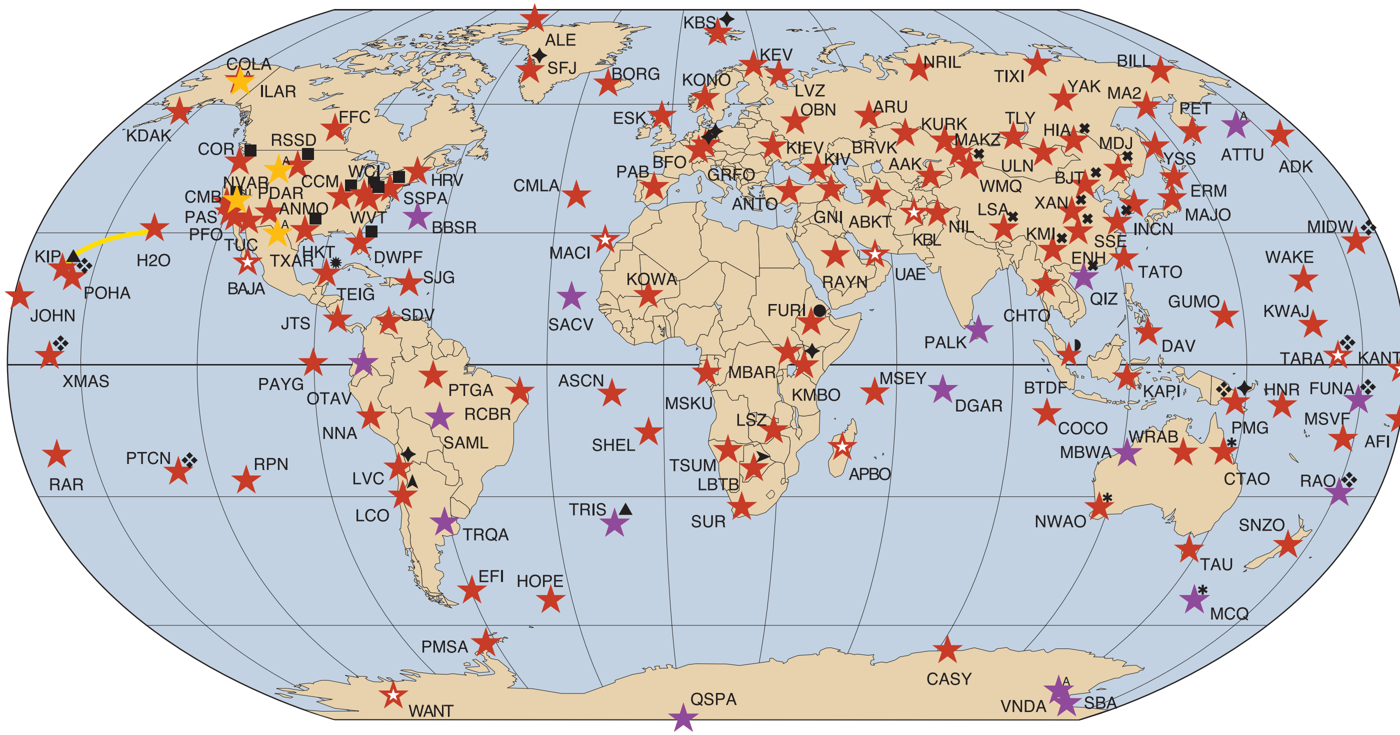

IRIS International & National Cooperative Sites

IRIS Current	Affiliate Array	Geoscope	Japan	Mednet	Geofon/AWI/BGR/BFO	China/USGS	Mexico	Singapore	Botswana	Andes	Austrailia	ANSS	AFTAC	SMU
★	★	★	★	★	★	★	★	★	★	★	★	★	★	★

Current GSN station coverage of Earth is shown as of August 2005. Sites added in the past five years are noted in purple (stations) and orange (arrays). Sites planned to be completed are noted with white stars. Cooperative sites are indicated by symbols on the upper right "shoulder" of the stars.


STS-1 Seismometer
at Harvard, Mass.

Global network record section for an earthquake off the coast of Jalisco, Mexico

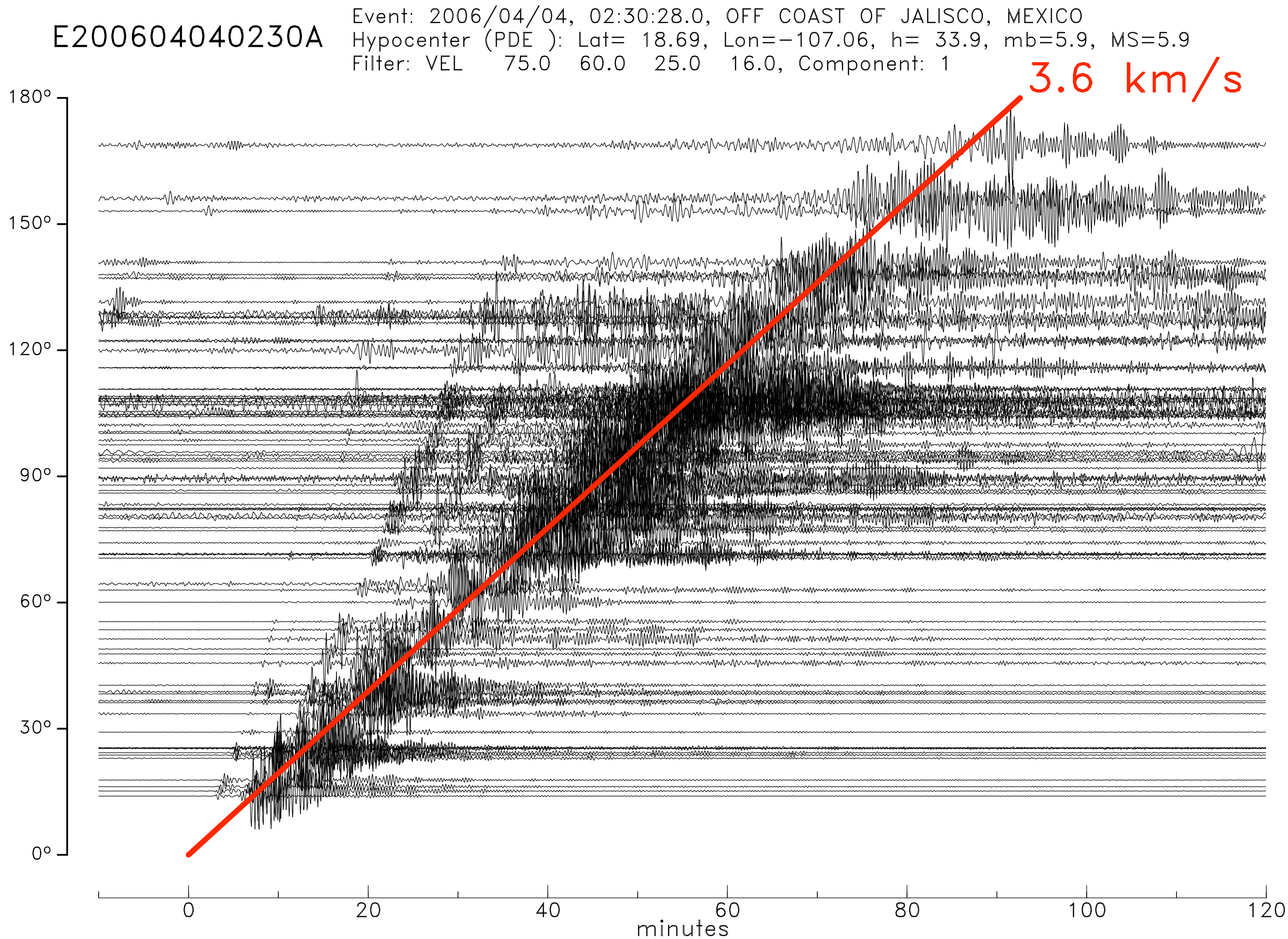

Moment-tensor analysis by waveform fitting

(Observed seismogram)/(Instrument response) x Filter = Observed waveform

(Synthetic displacement seismogram) x Filter = Model waveform

Model waveform depends on:

1. Earthquake parameters
2. Earth structure

If the Earth structure and the earthquake location are known, the

Model waveform depends only on the six elements of the moment tensor,

M_{xx}, M_{yy}, M_{zz}, M_{xy}, M_{xz}, and M_{yz}

Minimize the difference [Observed waveform - Model waveform]^2

with respect to the moment tensor elements.

Seismogram Modeling

The k-*th* seismogram in a data set for a given earthquake can be represented by:

$$u_k(\boldsymbol{r}, t) = \sum_{i=1}^{N} \psi_{ik}(\boldsymbol{r}_0, \boldsymbol{r}, t) f_i$$

where ψ_{ik} are the excitation kernels and f_i are independent parameters of the source model.

f_1 = Mzz, f_2 =Myy, etc.; N=6

Seismogram Synthesis for a Moment-Tensor Source

The seismic displacement field can be calculated by superposition of the normal modes of the Earth (Gilbert, 1971):

$$u(\boldsymbol{x}, t) = \sum_k [1 - \exp[-\alpha_k(t - t_s)] \cos \omega_k(t - t_s)] \, \boldsymbol{M} : \boldsymbol{e}^{(k)}(\boldsymbol{x}_s) \boldsymbol{s}_k(\boldsymbol{x})$$

where α_k is the decay constant of and $\boldsymbol{e}^k$ is the strain tensor in the k-*th* mode; $\boldsymbol{s}_k$ is the eigenfunction of the k-*th* mode; and $\boldsymbol{M}$ is the seismic moment tensor.

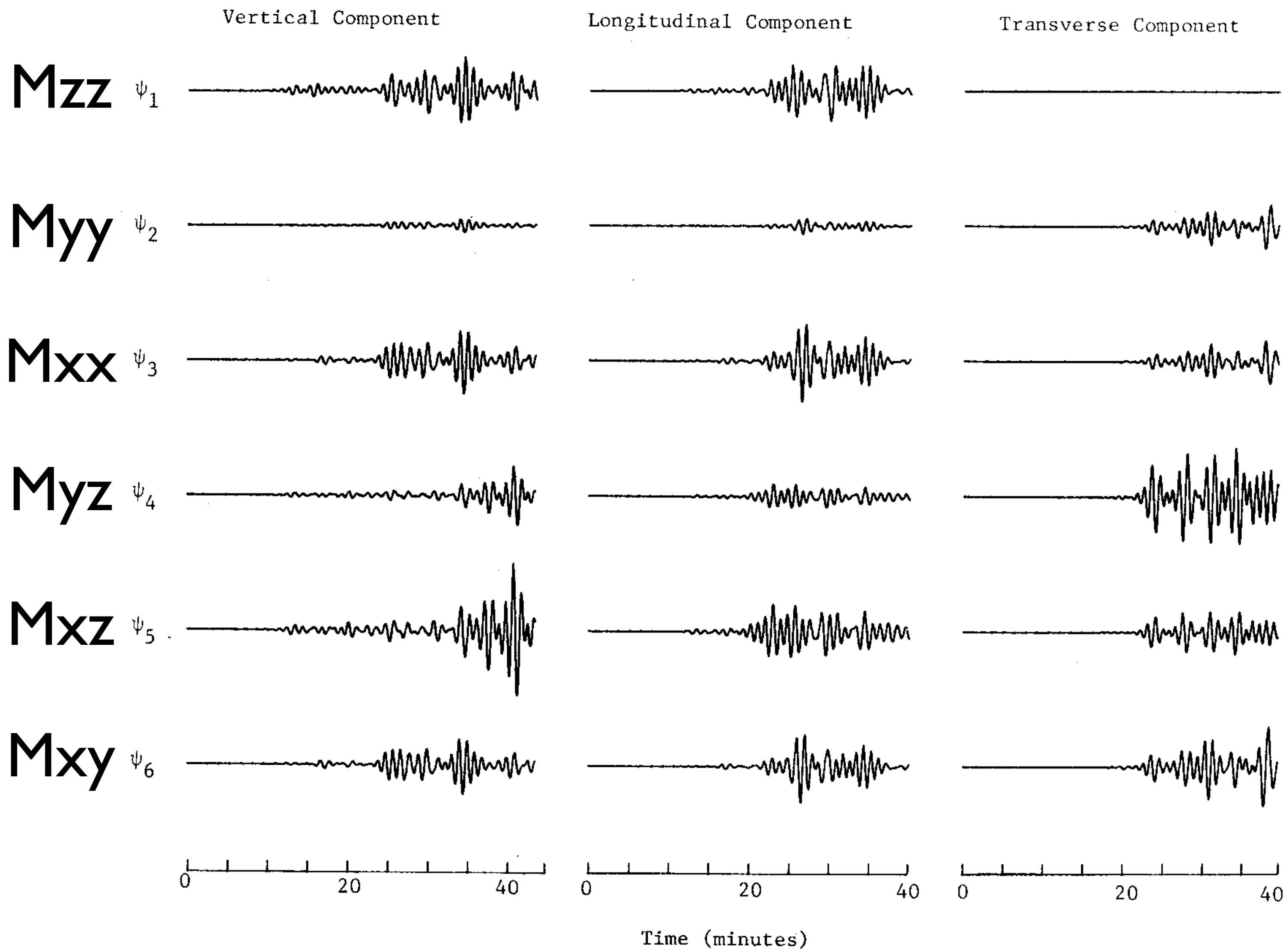

Excitation kernels for deep earthquake (580 km)

Fit to seismograms:
Body waves at Eskdalemuir, Scotland

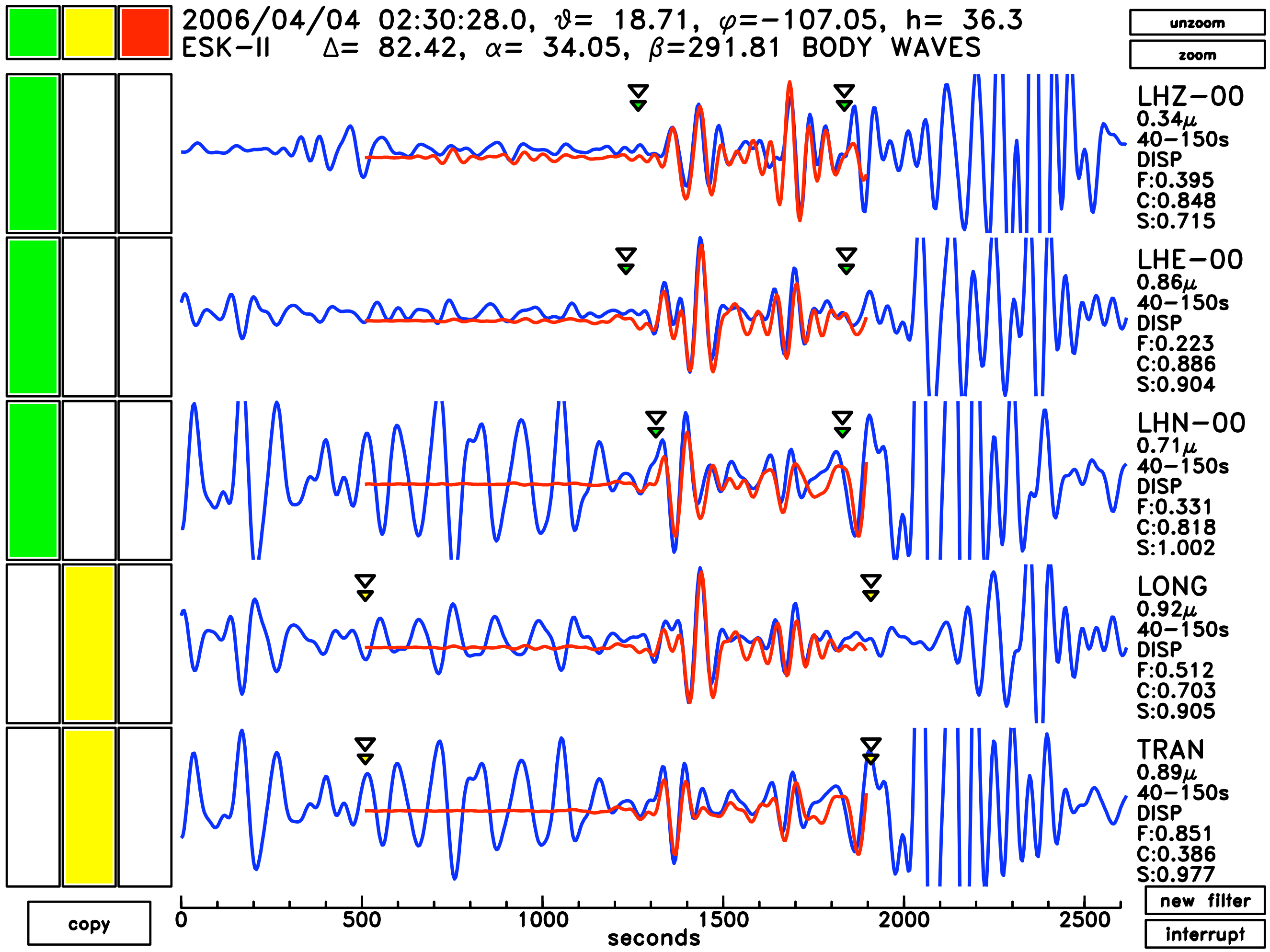

blue - data ; red - model

Fit to seismograms:
Surface waves at Hockley, Texas

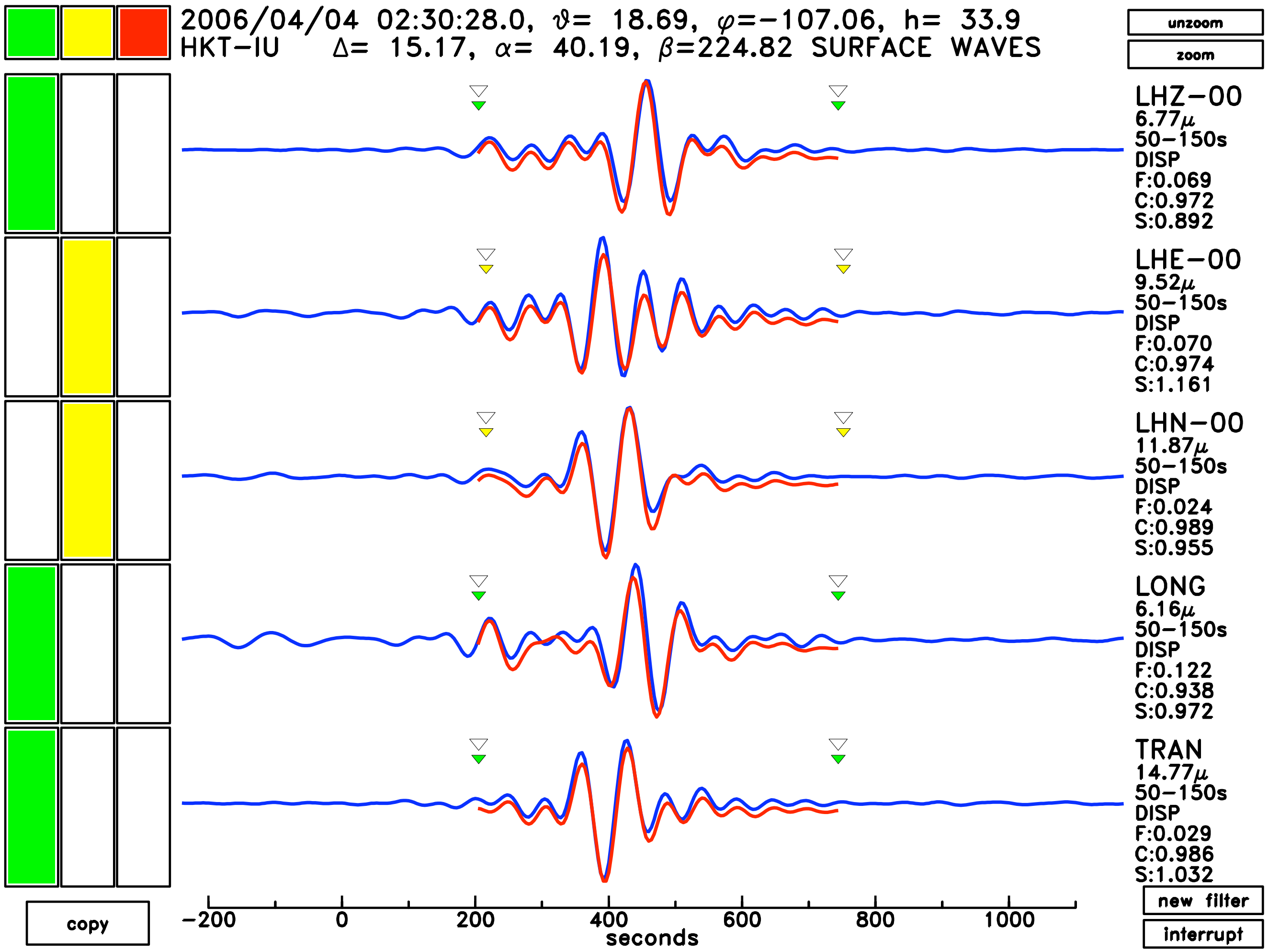

blue - data ; red - model

Estimation of the Source Parameters

For a point source, the elements f_i can be estimated by solving $\mathbf{A} \cdot \mathbf{f} = \mathbf{b}$, where:

$$A_{ij} = \sum_k \int_{t_{k_1}}^{t_{k_2}} \psi_{ik} \psi_{jk} dt \; ; \; b_j = \sum_k \int_{t_{k_1}}^{t_{k_2}} u_k \psi_{jk} dt.$$

This procedure requires that the position of the source $(\boldsymbol{r}_0, t_0)$ be known.

Solution for the Source Centroid

The earthquake centroid can be determined simultaneously with the source model parameters by expansion of the equations of condition to allow for a perturbation in the location of the source (Dziewonski, Chou and Woodhouse, 1981):

$$u_k = u_k^{(0)} + \{\psi_{ki,j}^{(0)} \cdot \delta x_j - \psi_{ki,t}^{(0)} \cdot \delta t_0\} \cdot f_i^{(0)} + \psi_{ki}^{(0)} \cdot \delta f_i \;;$$

where the superscript (0) indicates parameters determined for the starting location. The problem can then be solved iteratively.

Iterative procedure for moment-tensor source converges nicely

E200604040230A

Event: 2006/04/04, 02:30:28.0, OFF COAST OF JALISCO, MEXICO
Hypocenter (PDE): Lat= 18.71, Lon=-107.05, h= 36.3, mb=5.9, MS=5.9
Centroid : Lat= 18.80, Lon=-107.10, h= 24.2, MW=5.9

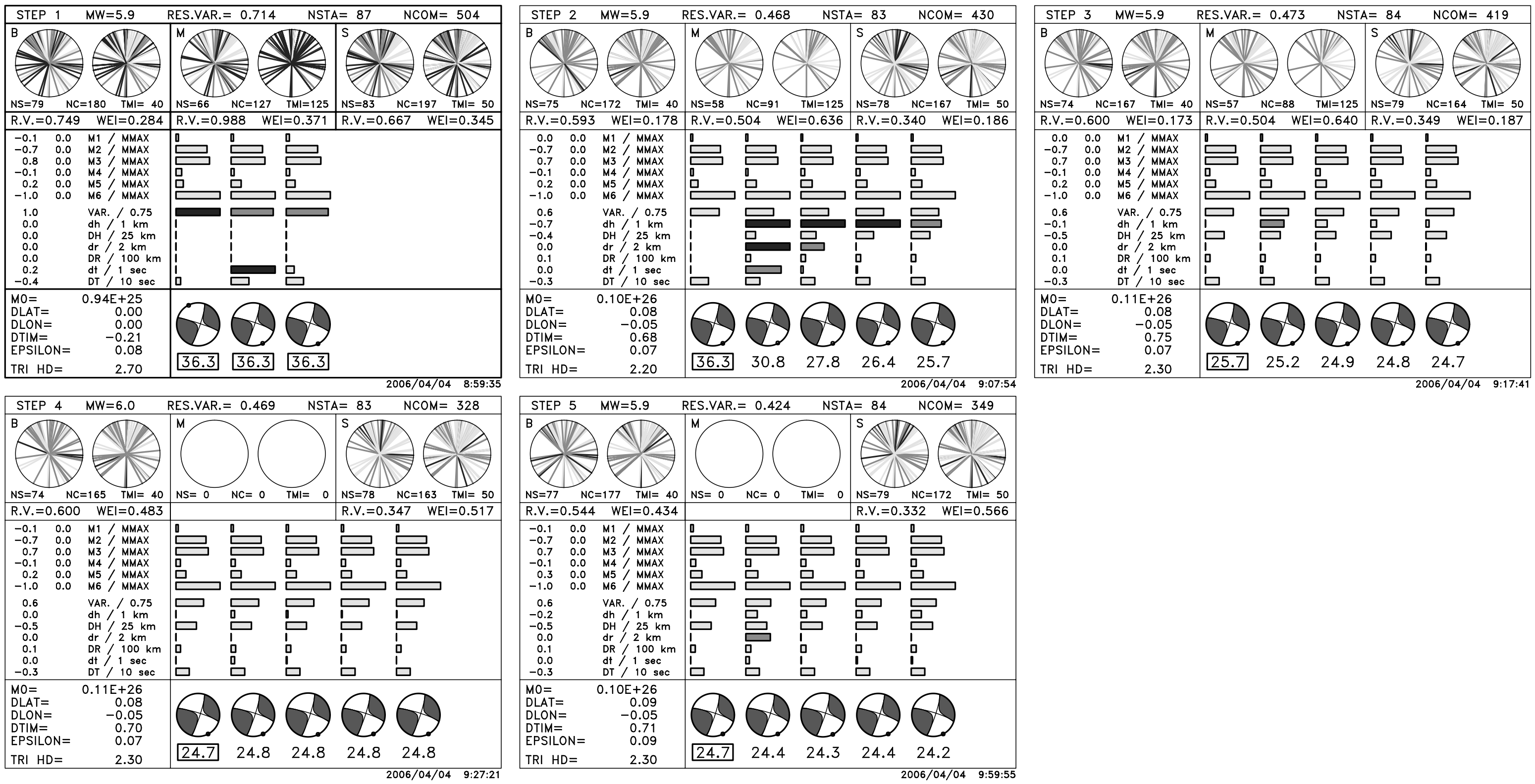

One week of quick CMTs

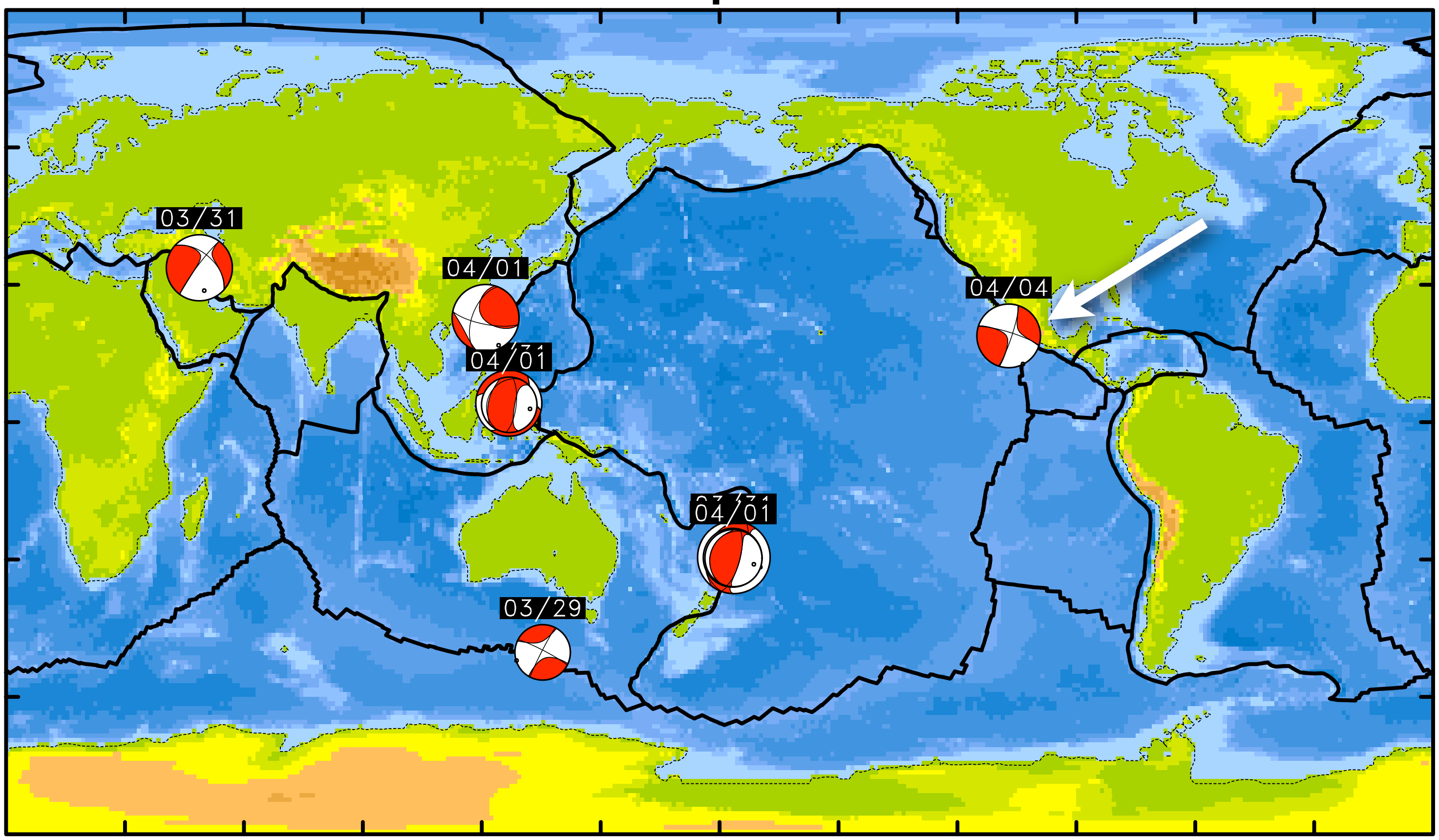

2. The Harvard (= Global) CMT catalog

3. Using calibration information in waveform analysis

4. Data quality control using noise

5. Data quality control using signals

6. Finding interesting things in the noise

The Harvard / Global CMT Project

Project started in 1981 (A.M. Dziewonski et al.)

Goal is (now) to determine source parameters for all earthquakes with M>5 worldwide

CMT catalog contains ~25,000 moment tensors for the period 1976-2006

In 2006 the project moved from Harvard University to Lamont/Columbia University

Shallow earthquakes, 1976-2006

(approximately 3000)

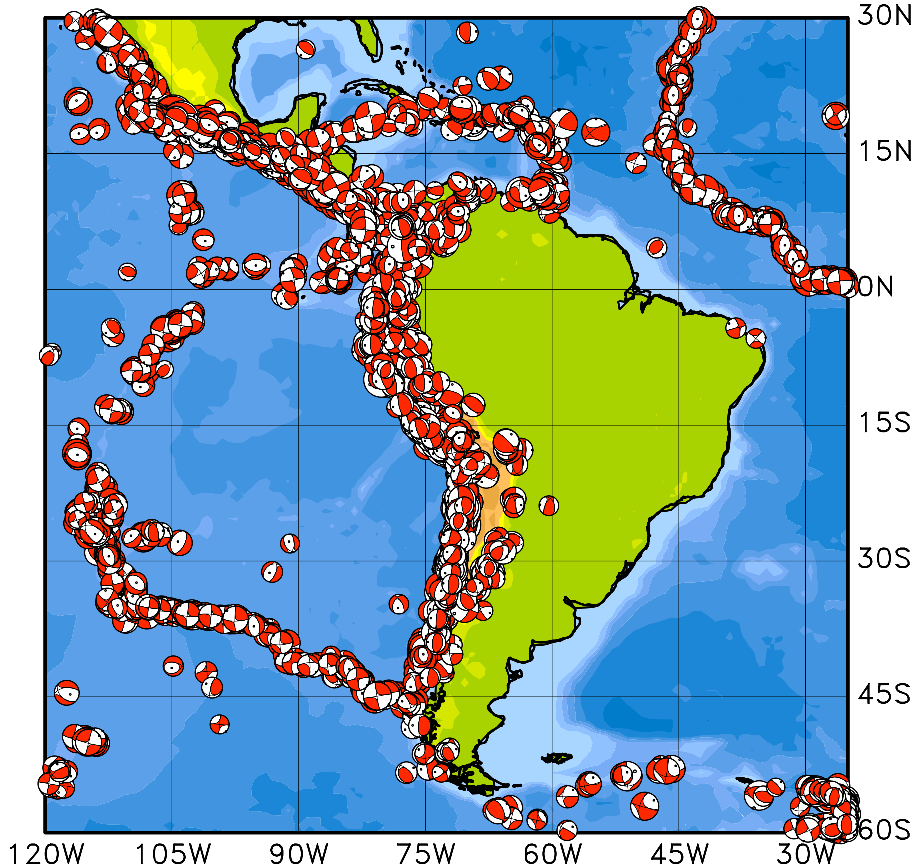

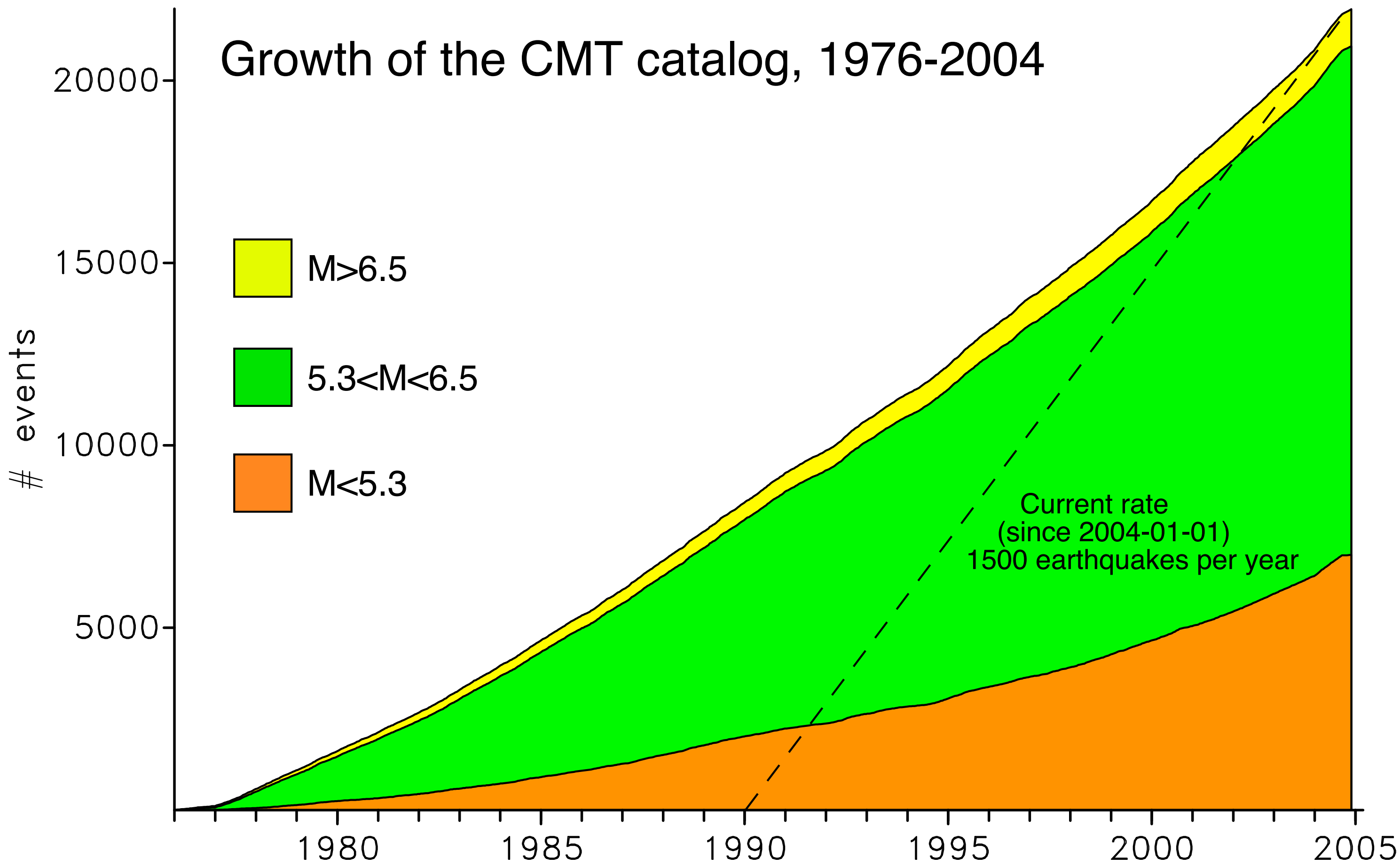

Growth of the CMT catalog, 1976-2004
M>6.5
5.3<M<6.5
M<5.3
Current rate
(since 2004-01-01)
1500 earthquakes per year
events
20000
15000
10000
5000
1980
1985
1990
1995
2000
2005

Cumulative moment release since 1976

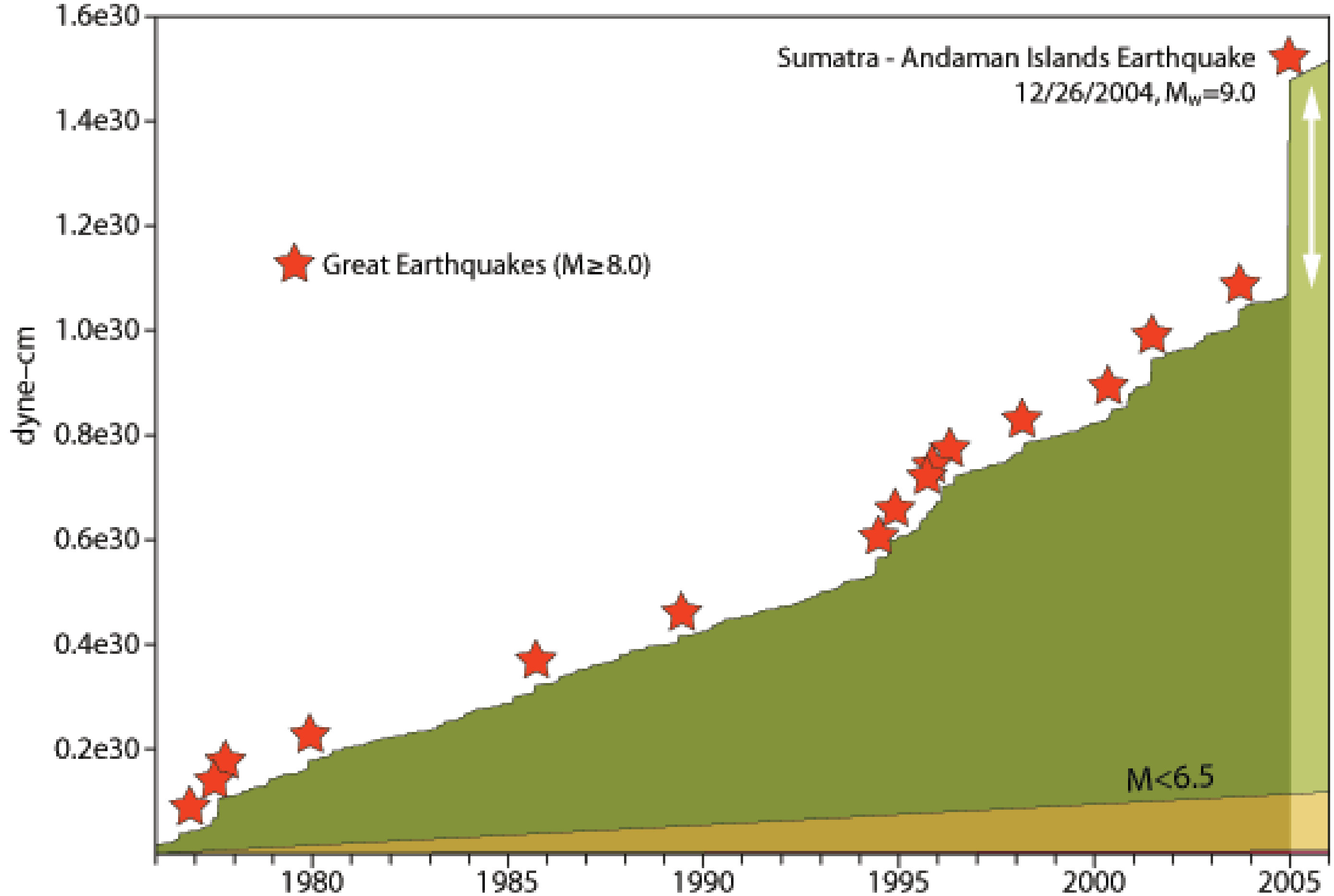

The CMT catalog can be accessed now at
www.seismology.harvard.edu

and soon at
www.globalcmt.org

3. Using calibration information in waveform analysis

4. Data quality control using noise

5. Data quality control using signals

6. Finding interesting things in the noise

The Global Digital Network in 1976

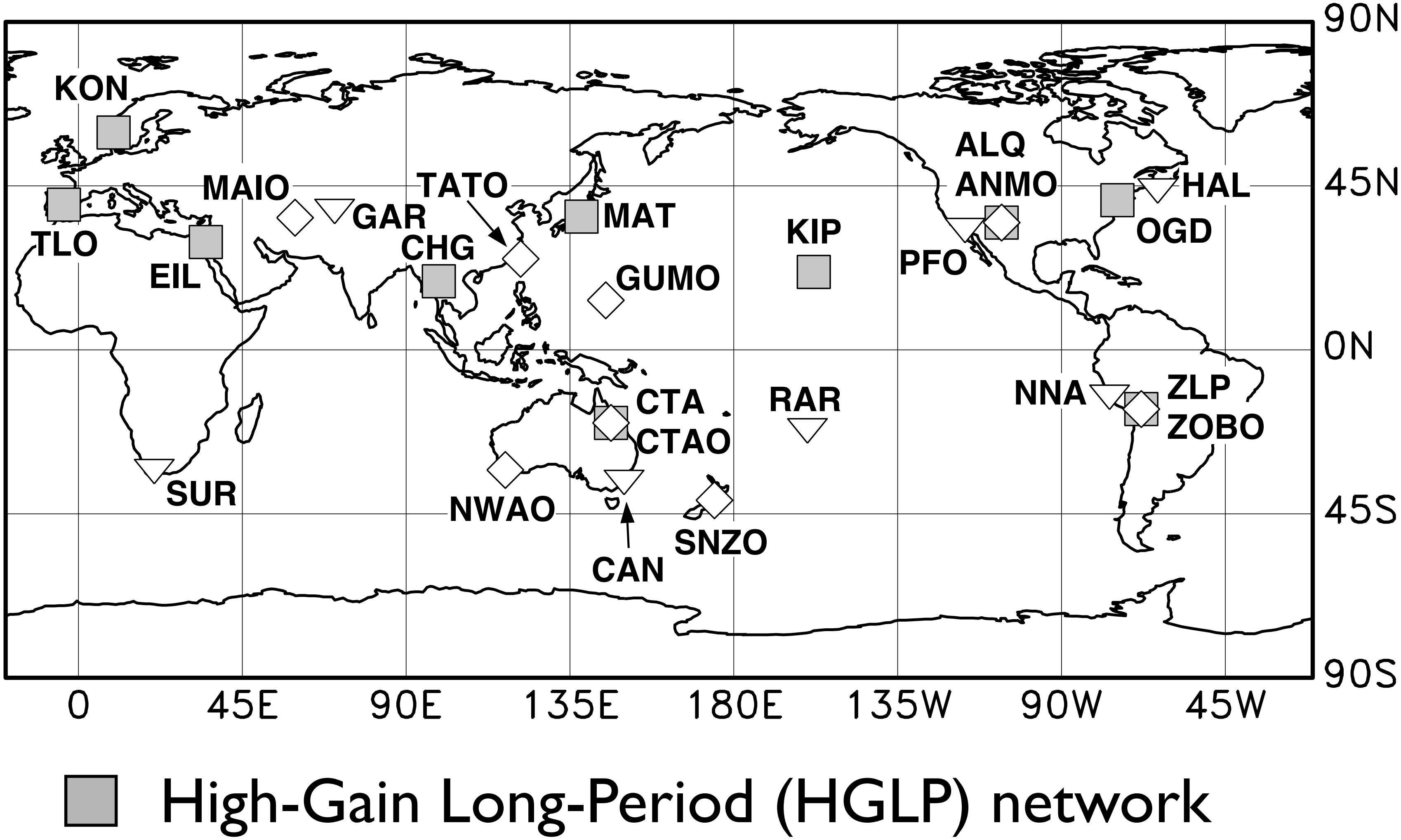

(Ekström and Nettles, PEPI, 1997)

HLGP seismometer and recording system

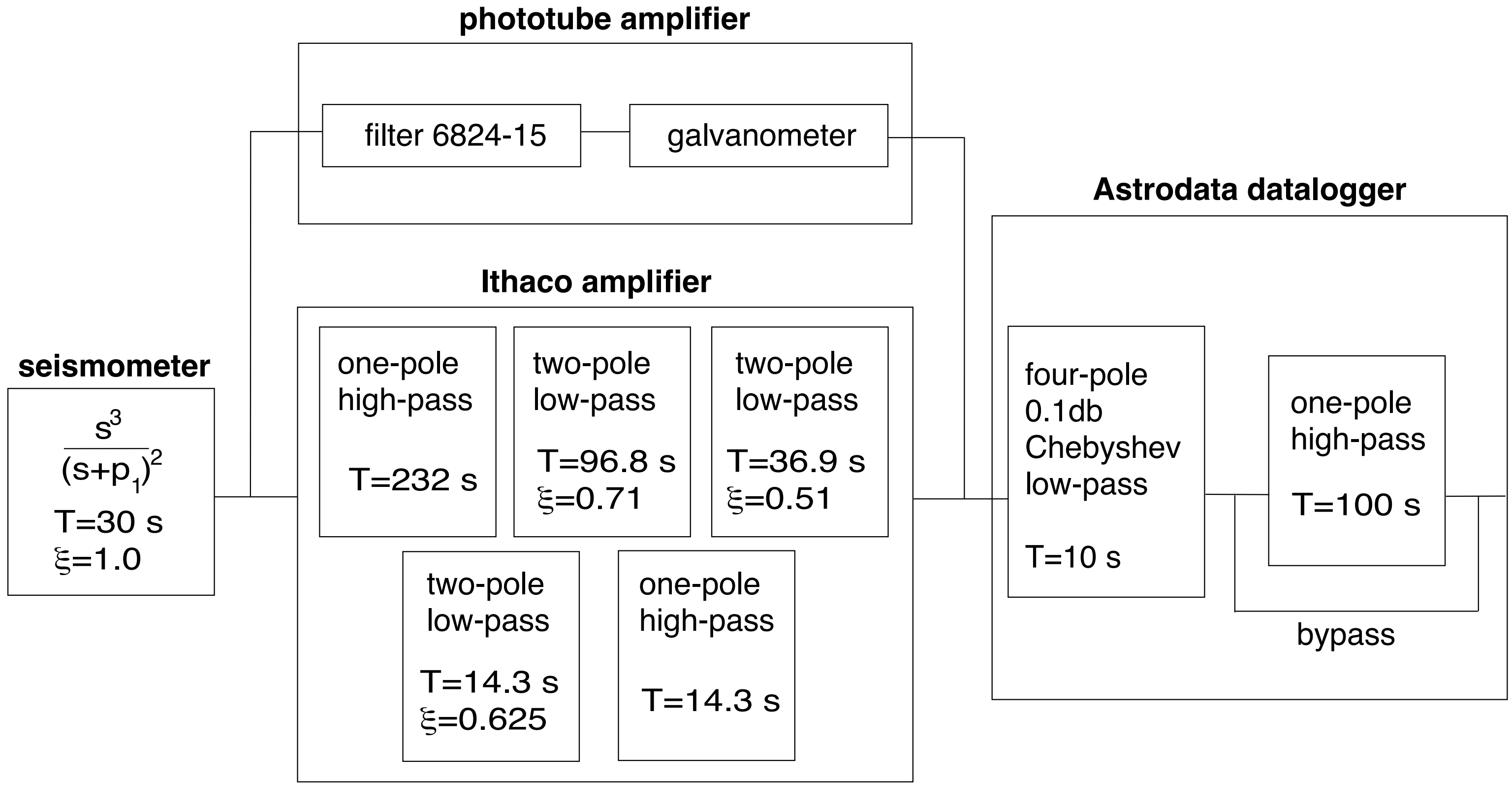

(Ekström and Nettles, PEPI, 1997)

Original calibration pulses and pulses for nominal response

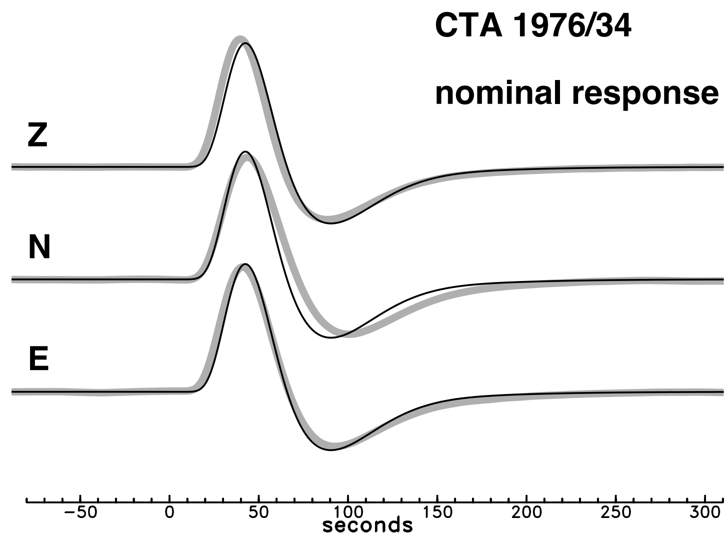

Original calibration pulses and pulses for new response after inversion

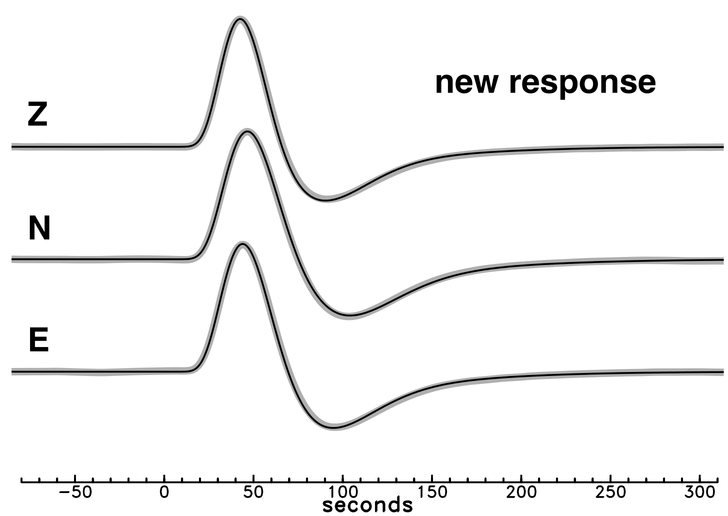

(Ekström and Nettles, PEPI, 1997)

Comparison of waveforms after normalizing responses for two stations in the same location

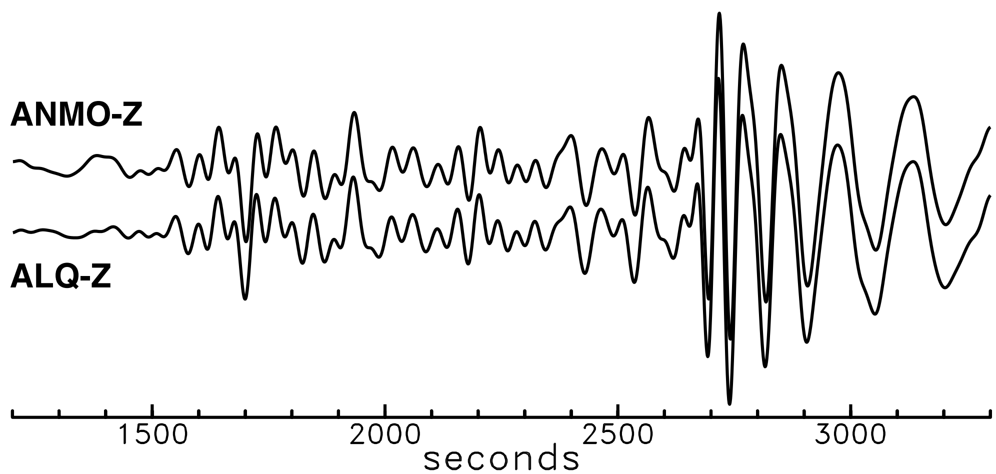

(Ekström and Nettles, PEPI, 1997)

Check of new responses -- sine-wave calibrations

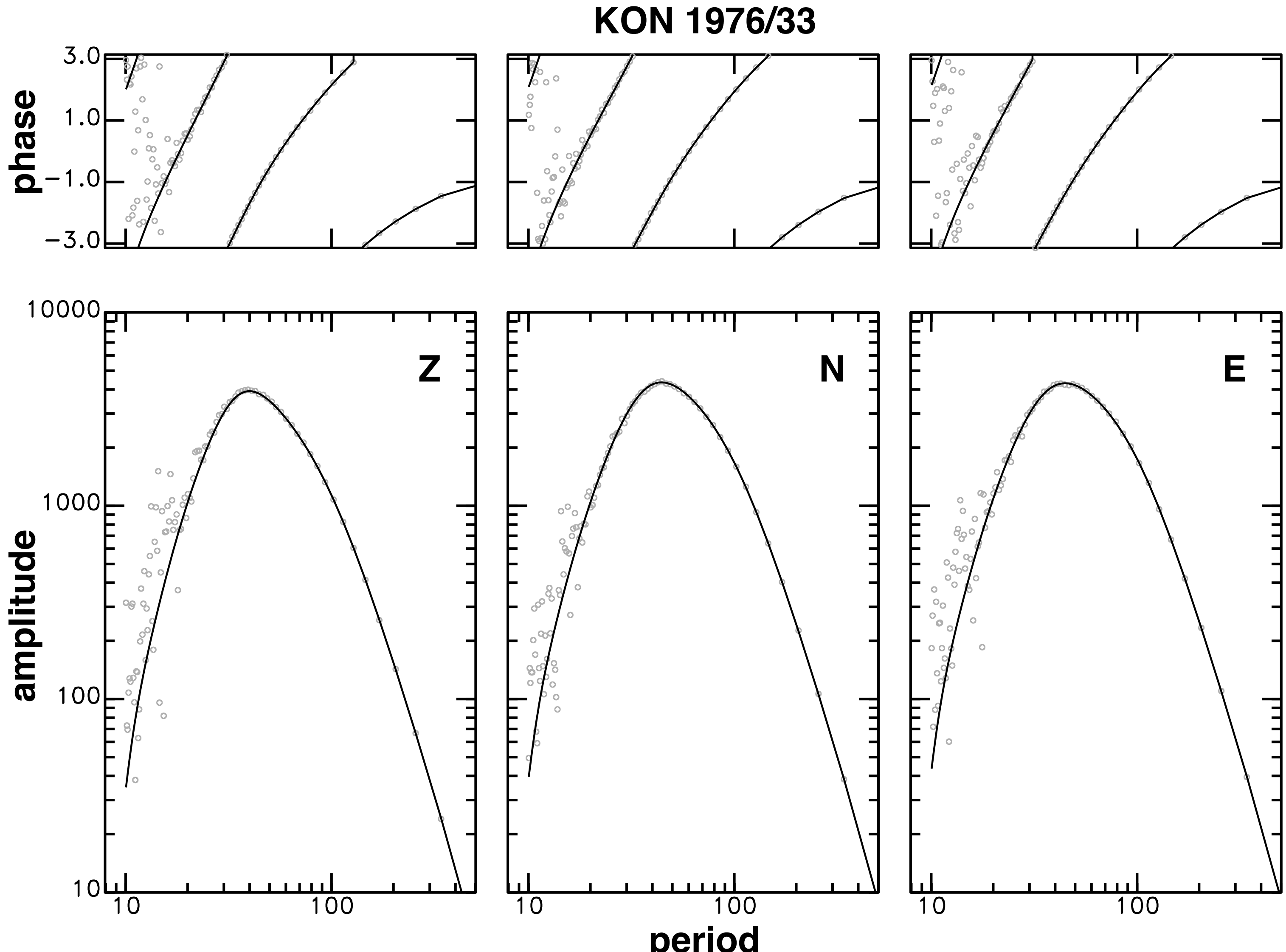

(Ekström and Nettles, PEPI, 1997)

Some channels were reversed for some periods of time

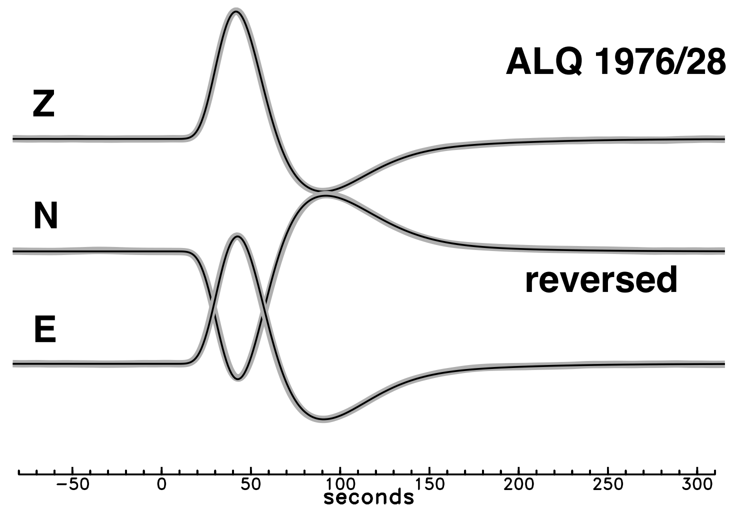

Some channels had extra filters for some periods of time

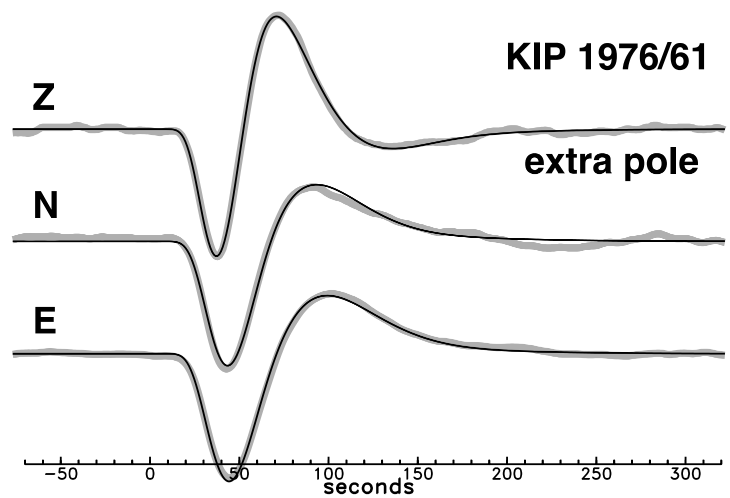

(Ekström and Nettles, PEPI, 1997)

Waveform comparisons (observed and synthetic) after correcting seismograms using new responses: The 1976 Friuli earthquake

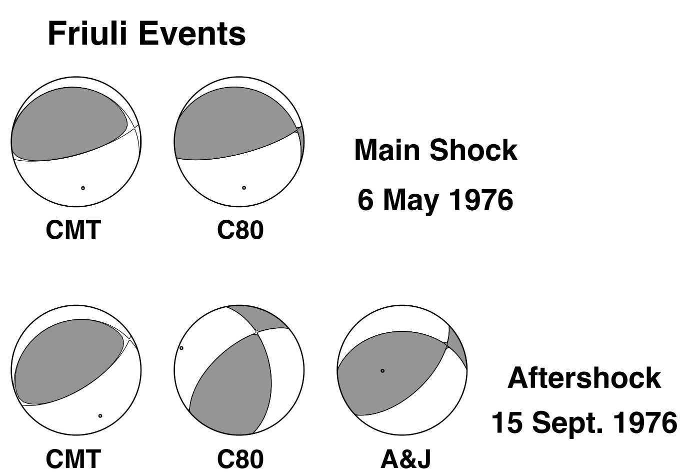

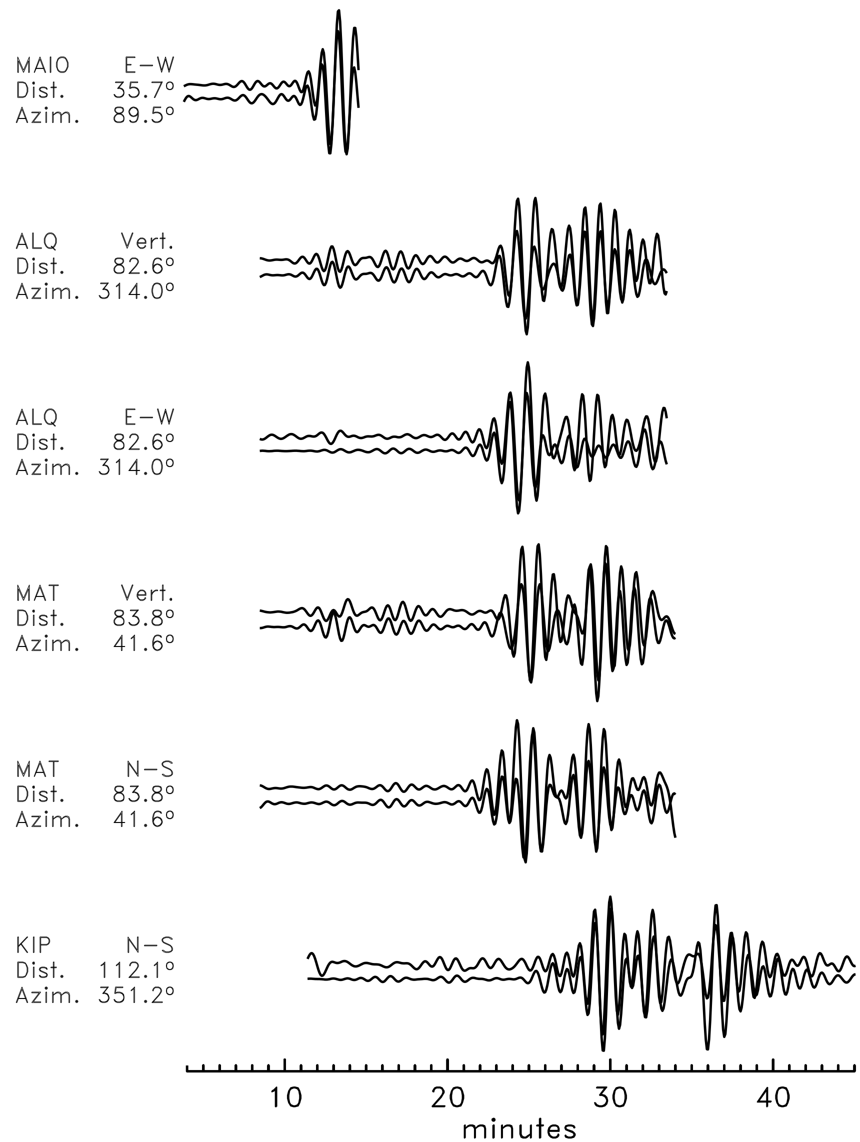

(Ekström and Nettles, PEPI, 1997)

4. Data quality control using noise

5. Data quality control using signals

6. Finding interesting things in the noise

Calculation of signal power of long-period GSN data

continuous filtered time series:

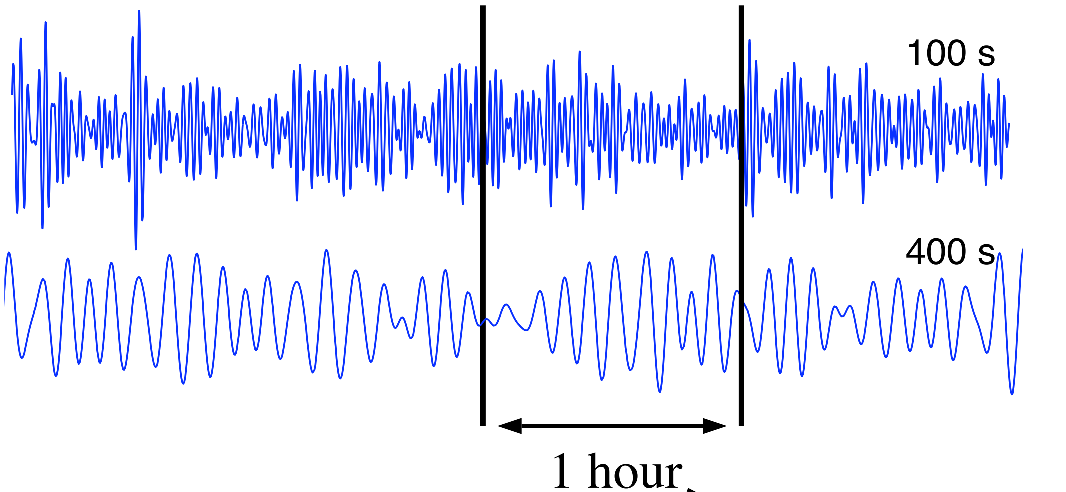

1. calculate rms
2. convert to power spectral density
3. store as hourly samples of signal level

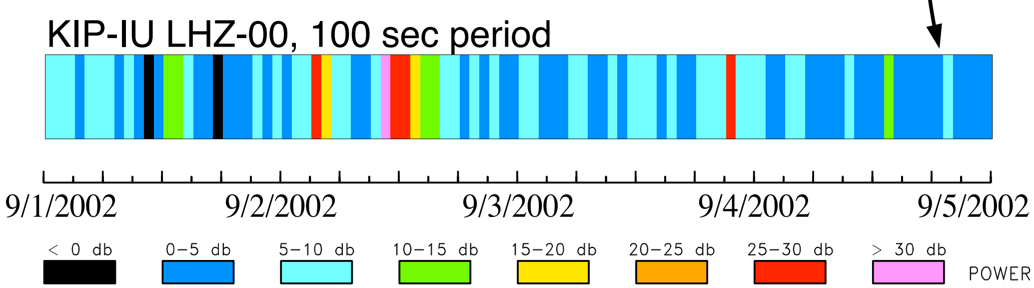

One week of noise at 23 seconds period

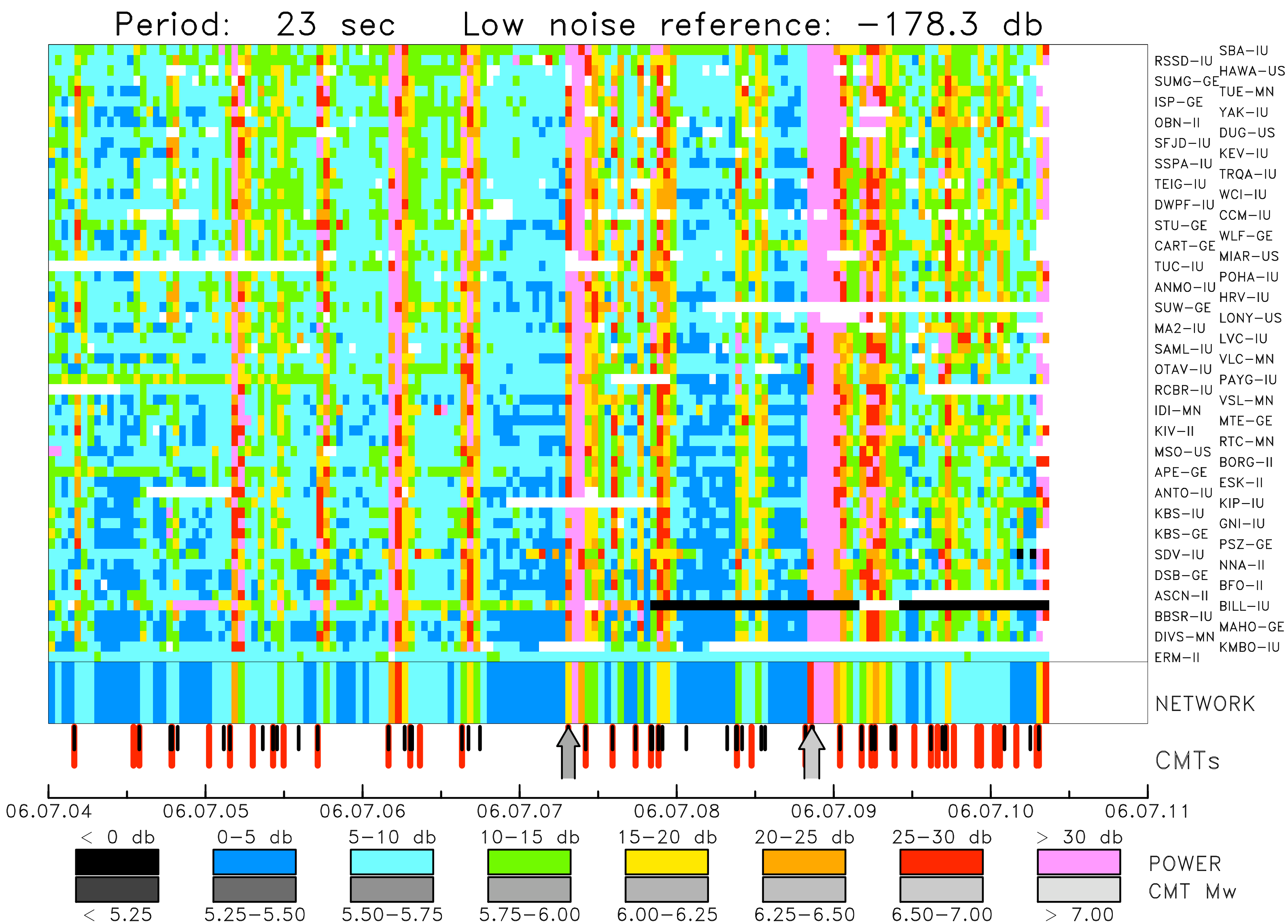

One week of noise at 100 seconds period

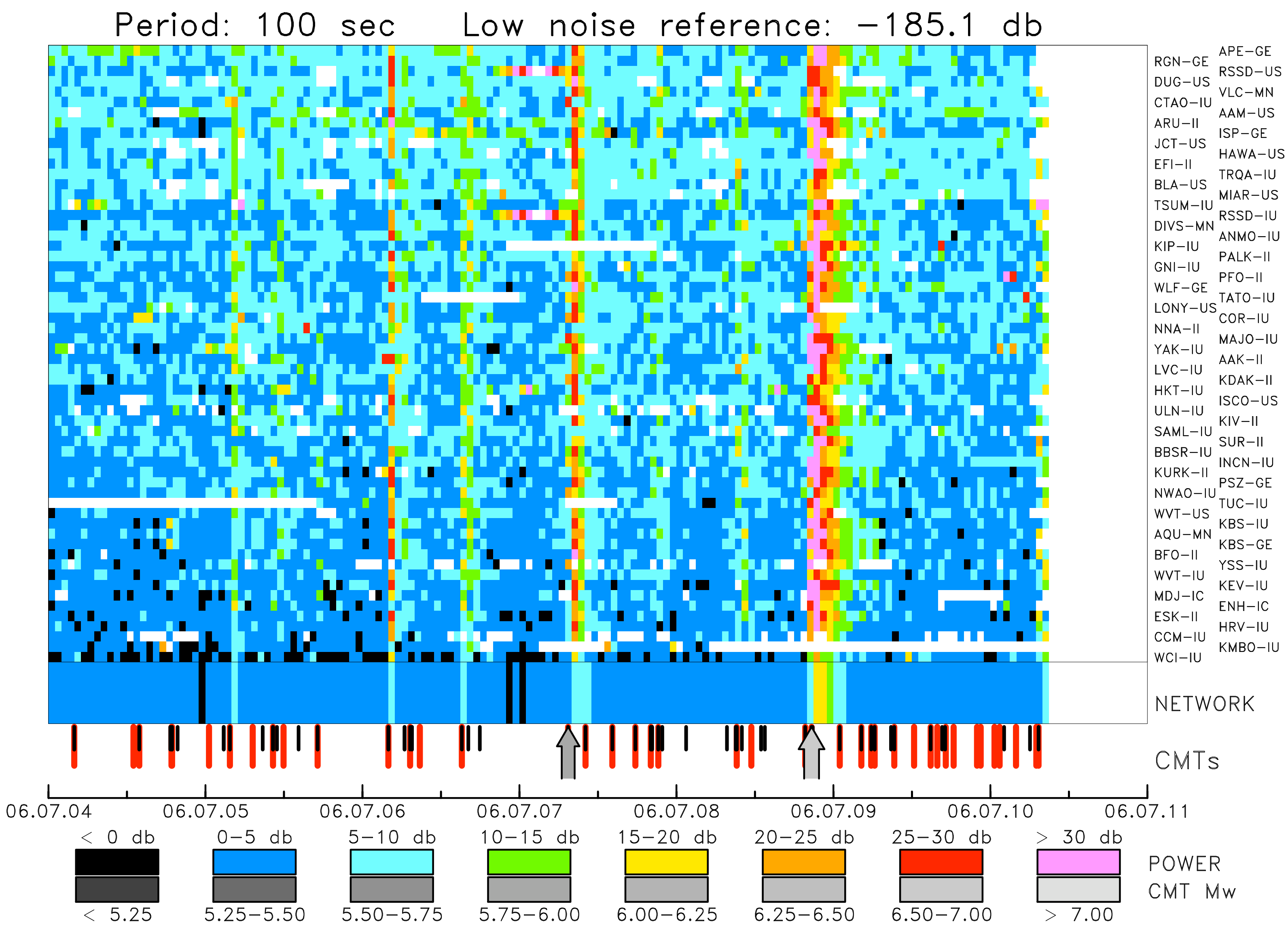

One week of noise at 228 seconds period

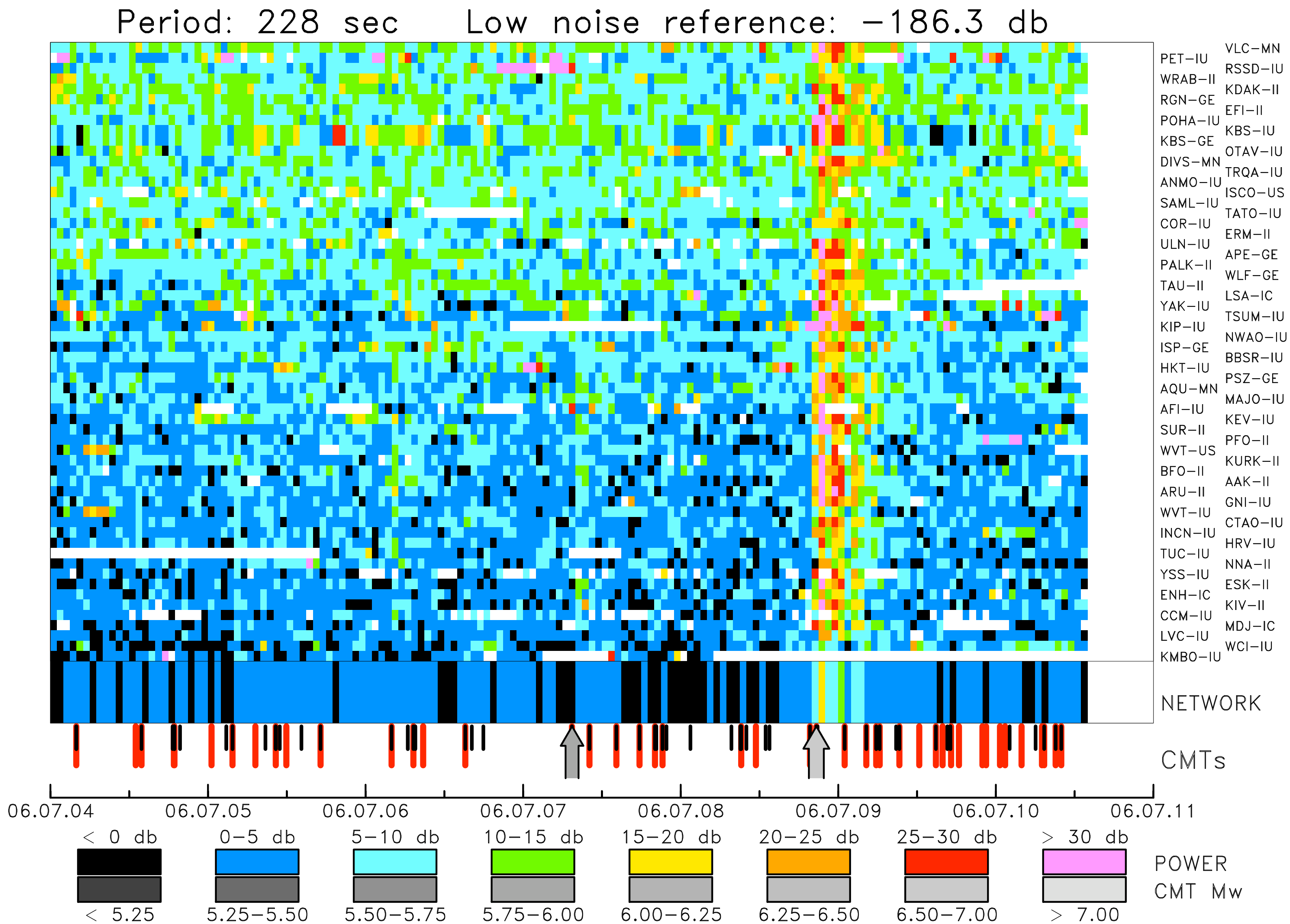

100 sec period - distribution of PSD

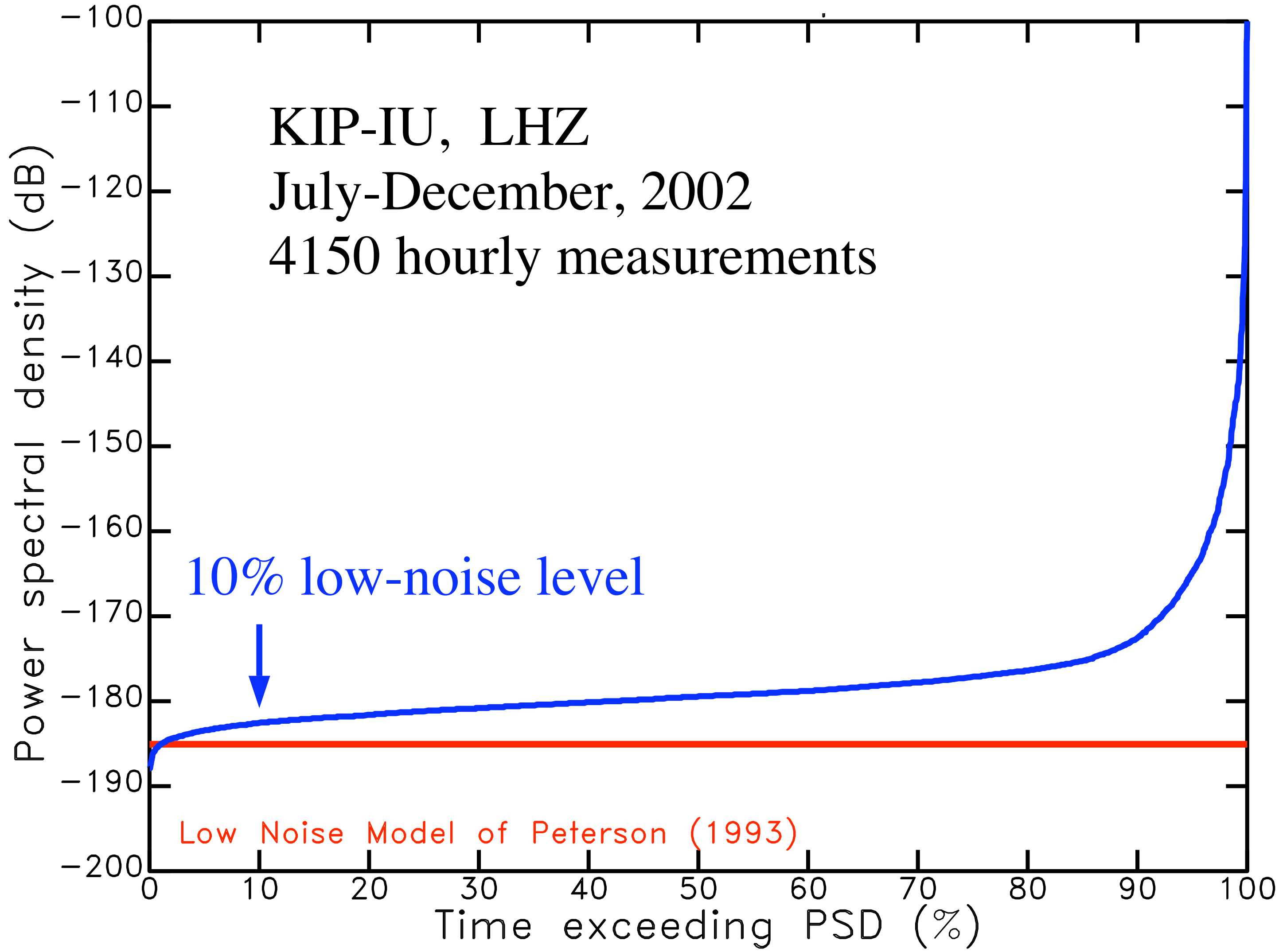

Noise spectra from the Global Seismic Network

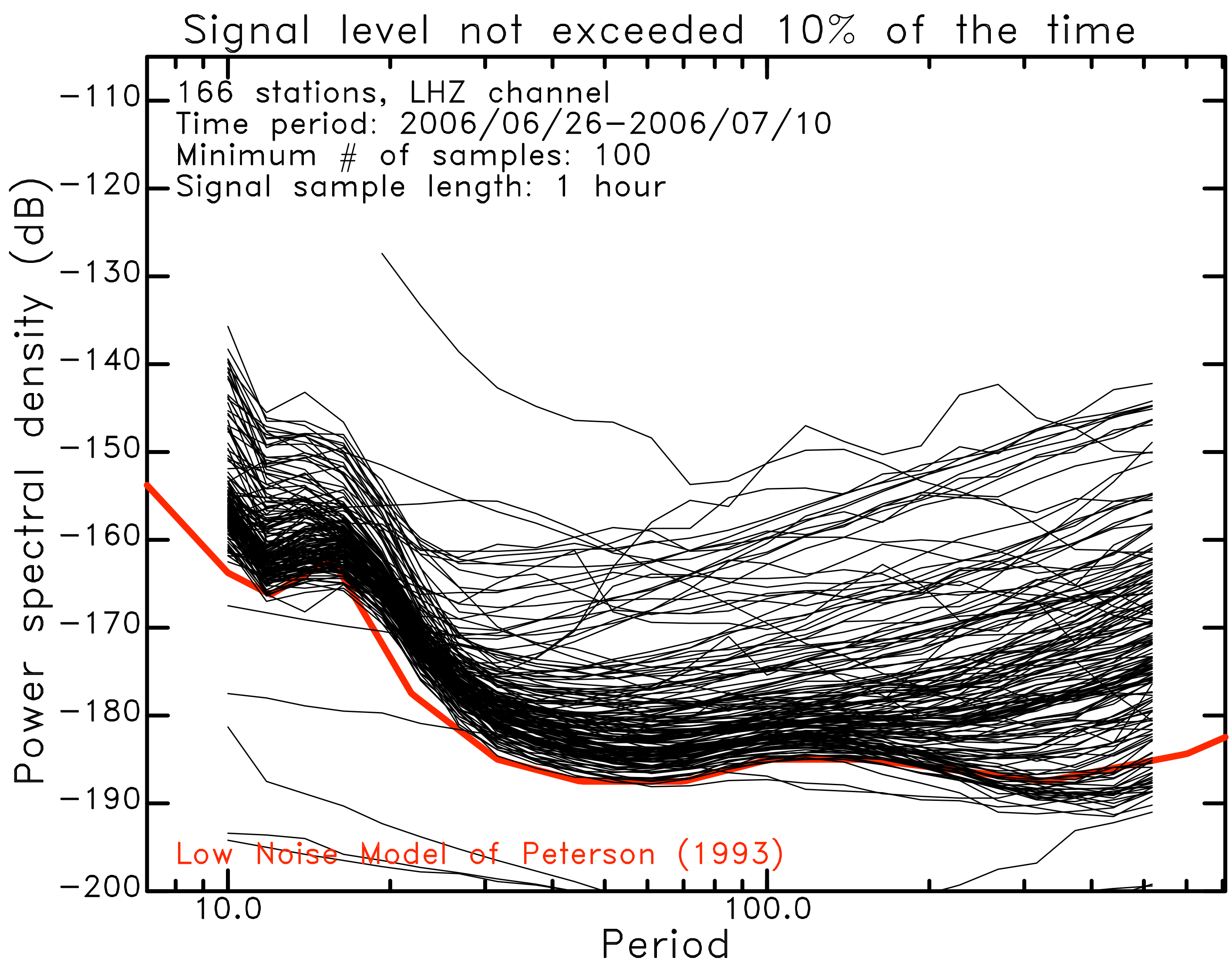

Stability of low-noise spectra

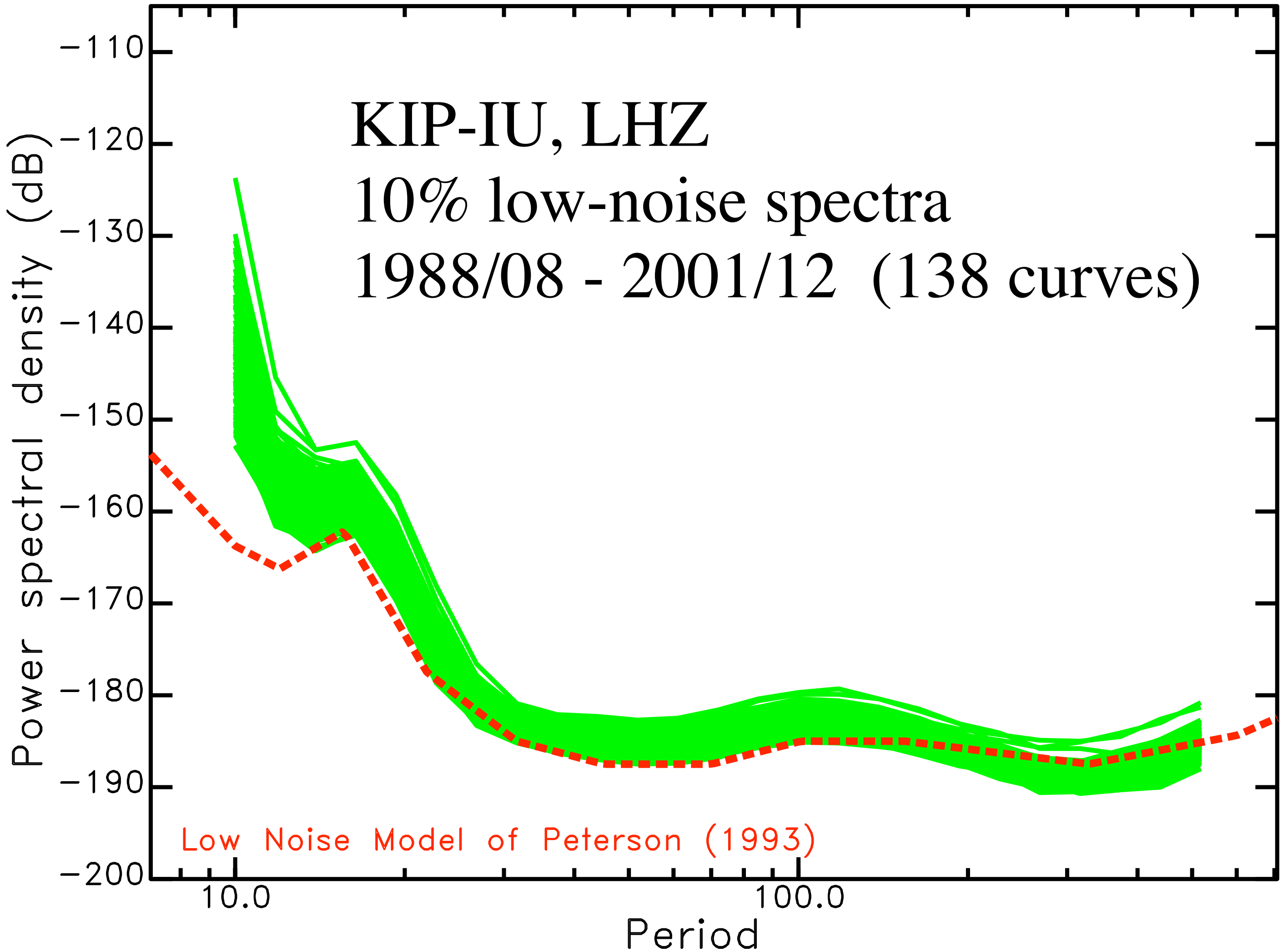

10% low-noise level at KIP since 1988

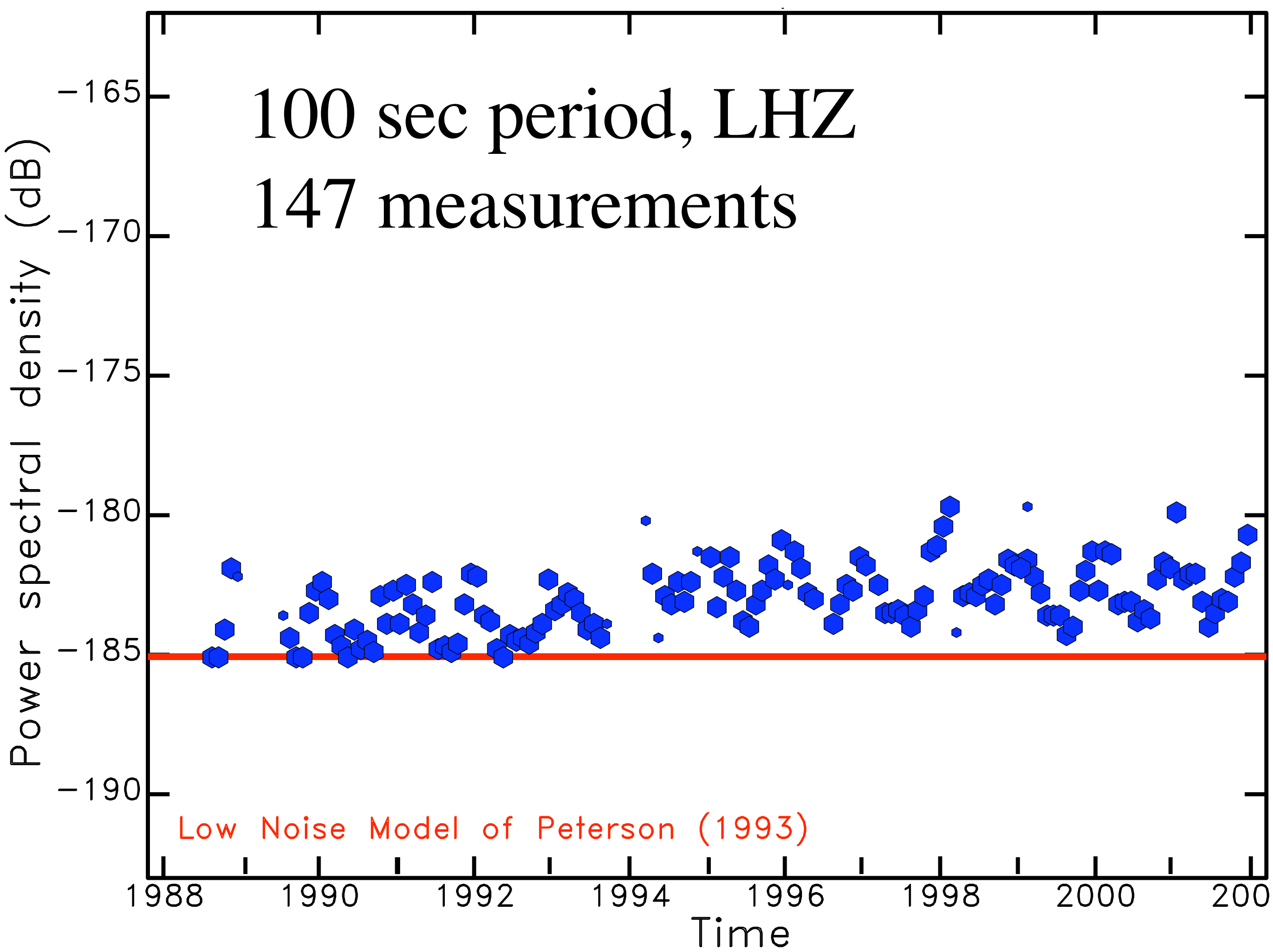

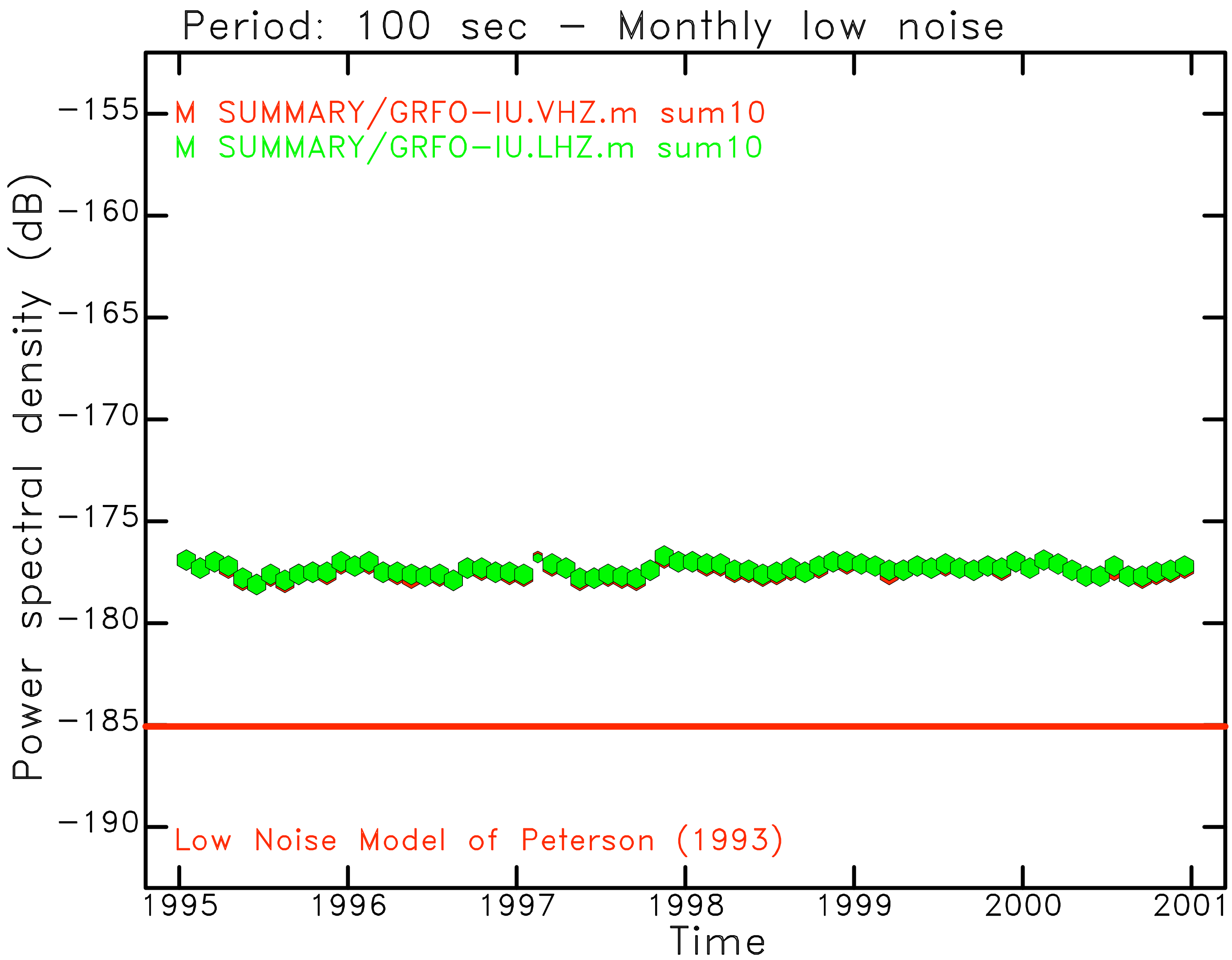
Period: 100 sec – Monthly low noise
M SUMMARY/GRFO-IU.VHZ.m sum10
M SUMMARY/GRFO-IU.LHZ.m sum10
Low Noise Model of Peterson (1993)
Power spectral density (dB)
−155
−160
−165
−170
−175
−180
−185
−190
1995
1996
1997
1998
1999
2000
2001
Time

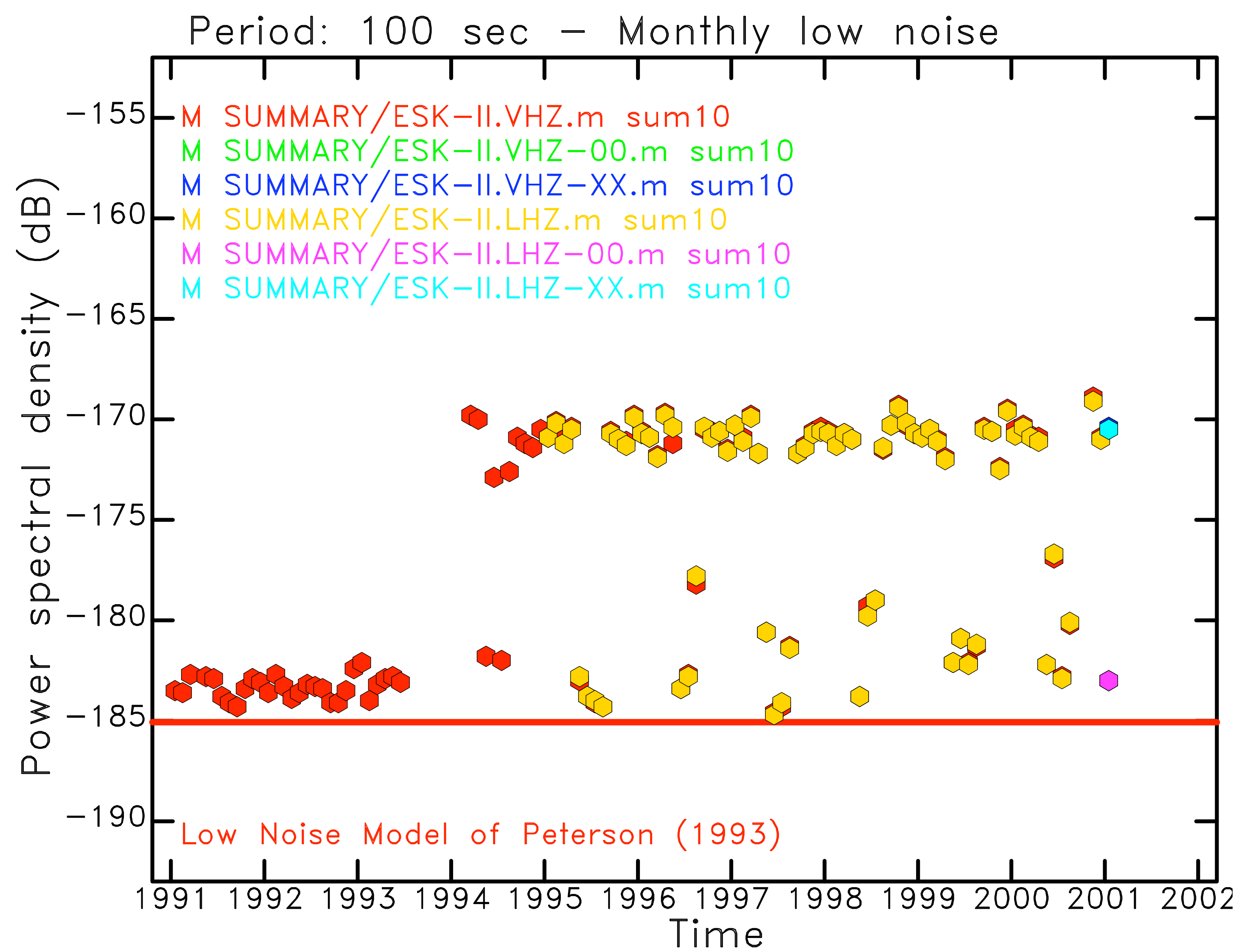

Period: 100 sec - Monthly low noise
M SUMMARY/ESK-II.VHZ.m sum10
M SUMMARY/ESK-II.VHZ-00.m sum10
M SUMMARY/ESK-II.VHZ-XX.m sum10
M SUMMARY/ESK-II.LHZ.m sum10
M SUMMARY/ESK-II.LHZ-00.m sum10
M SUMMARY/ESK-II.LHZ-XX.m sum10
Low Noise Model of Peterson (1993)
Power spectral density (dB)
-155
-160
-165
-170
-175
-180
-185
-190
1991
1992
1993
1994
1995
1996
1997
1998
1999
2000
2001
2002
Time

5. Data quality control using signals

6. Finding interesting things in the noise

Blue - observed seismograms

Red - synthetic seismograms

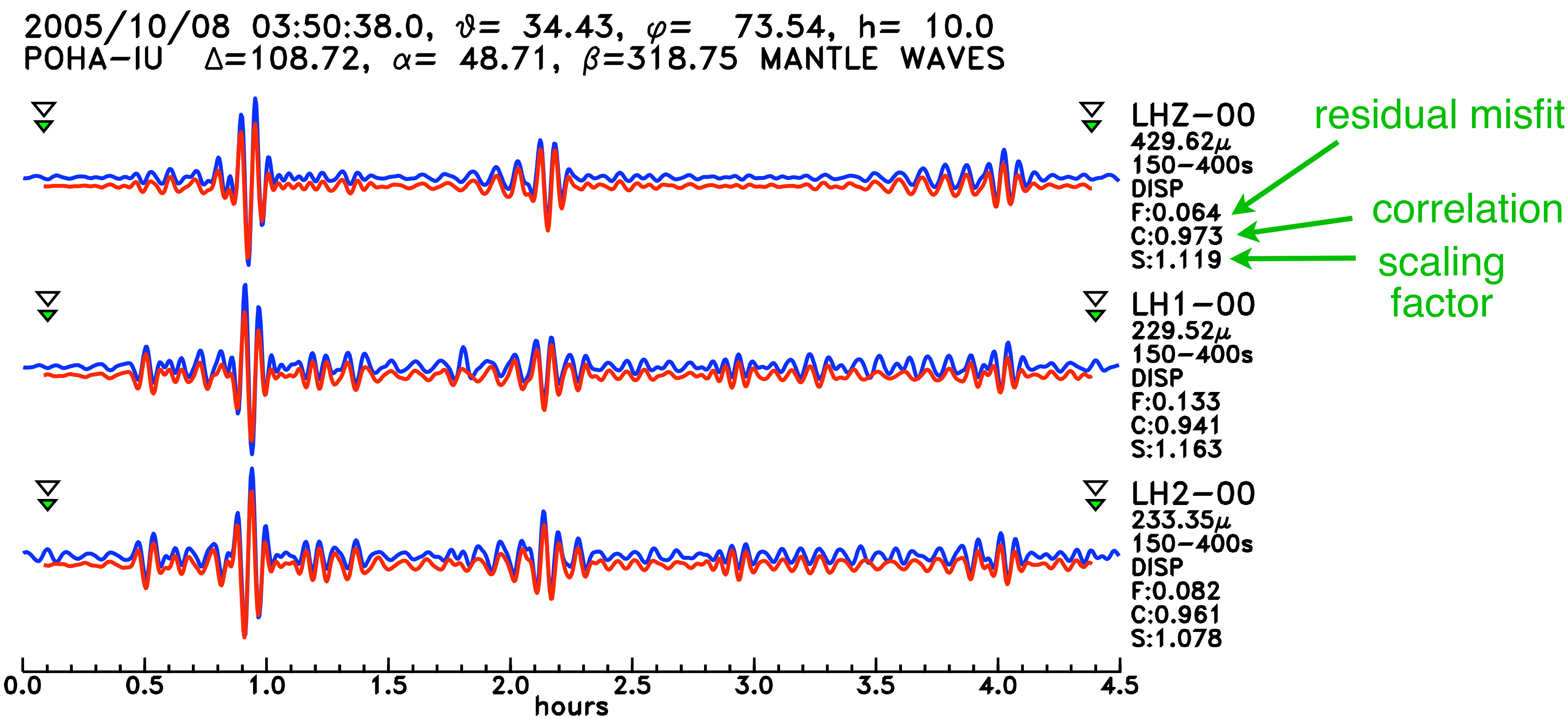

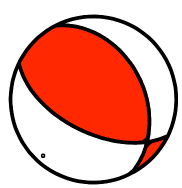

$$S = \frac{\sum_{i=1}^{N} o_i s_i}{\sum_{i=1}^{N} s_i^2}$$

Blue - observed seismograms

Red - synthetic seismograms

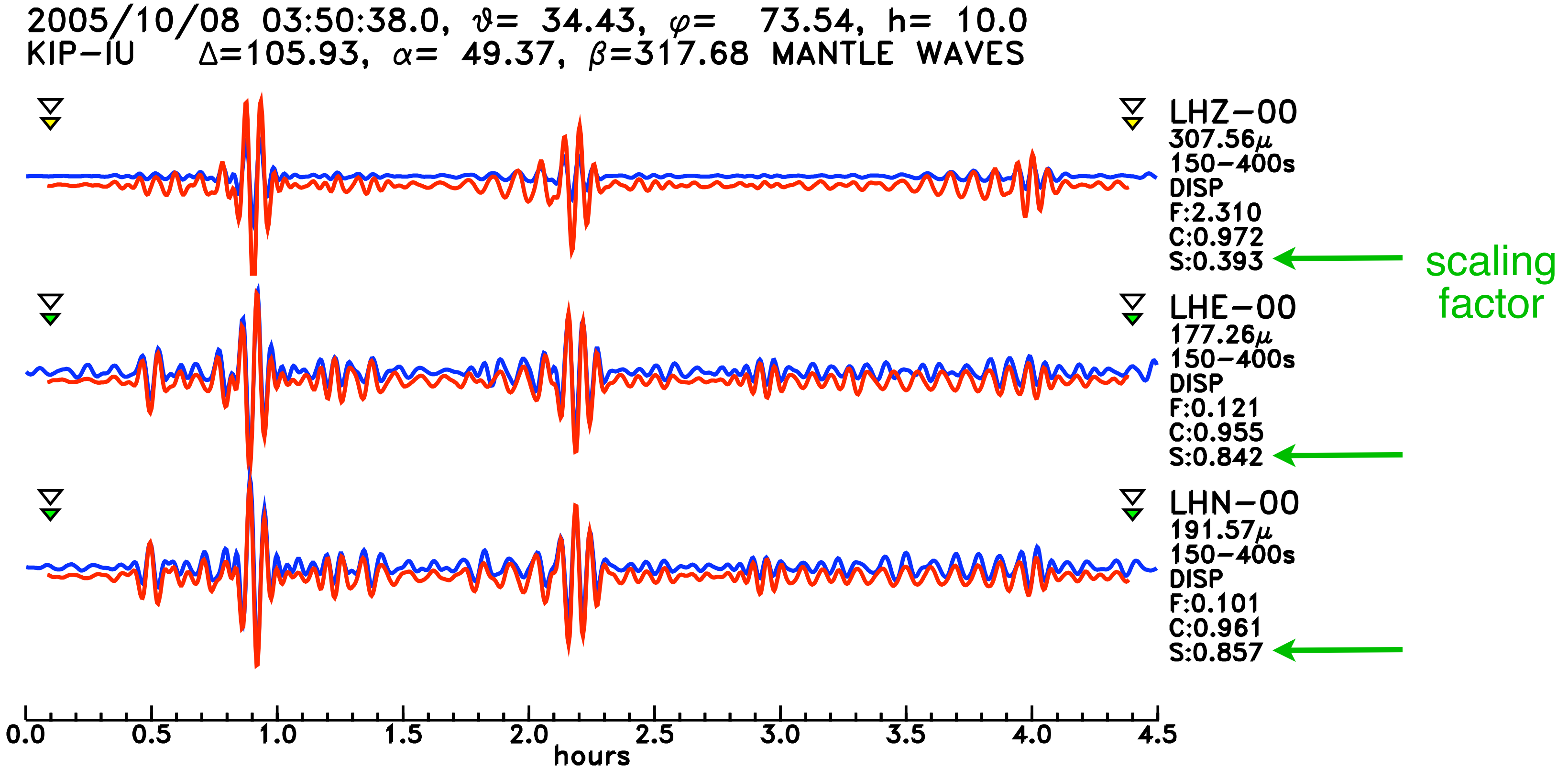

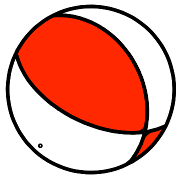

$$\boxed{S = \frac{\sum_{i=1}^{N} o_i s_i}{\sum_{i=1}^{N} s_i^2}}$$

Scaling factors at NNA-II, 1990-2004

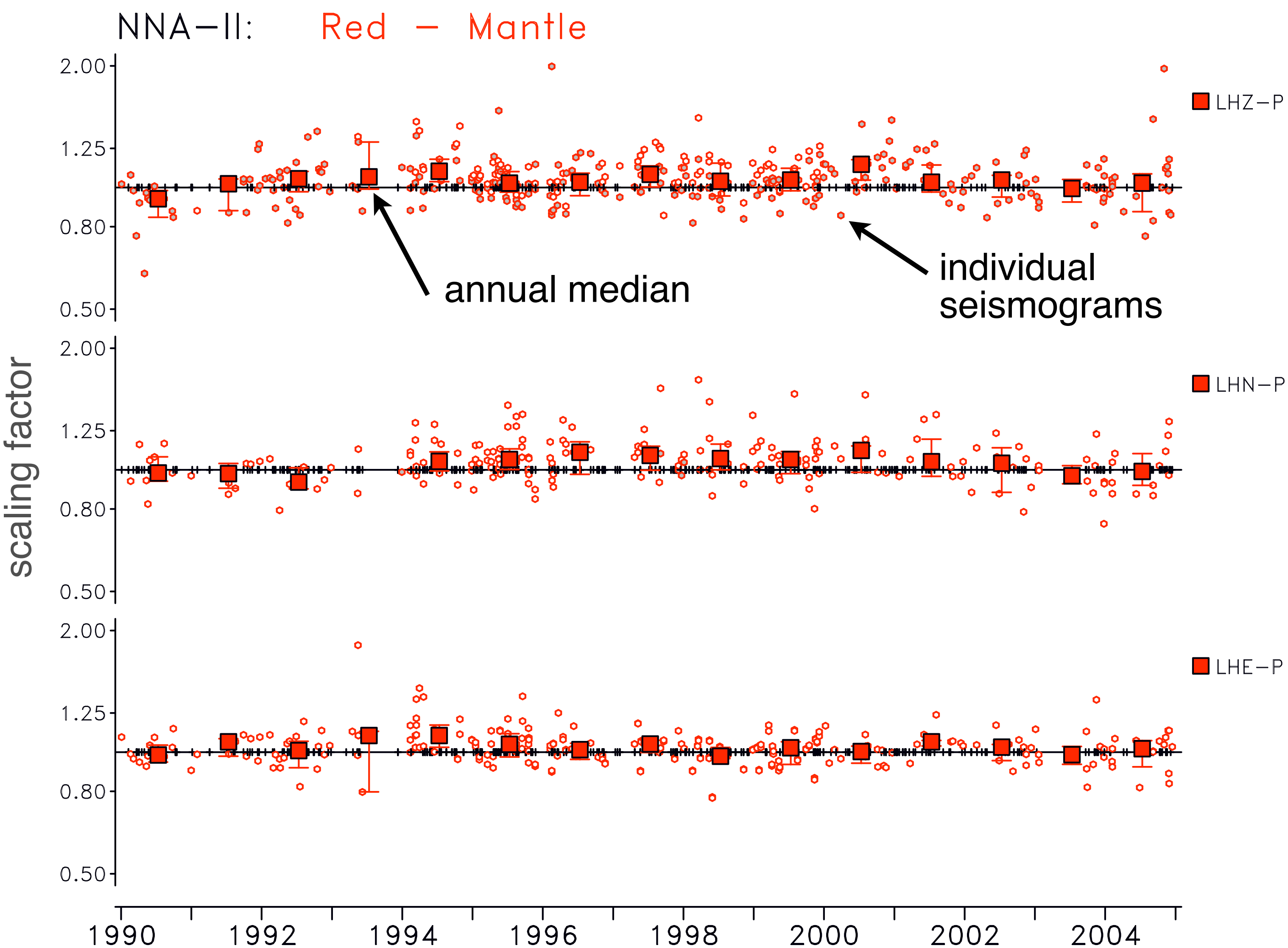

(Ekström, Dalton, and Nettles, SRL, 2006)

Scaling factors at ANMO-IU, 1990-2004

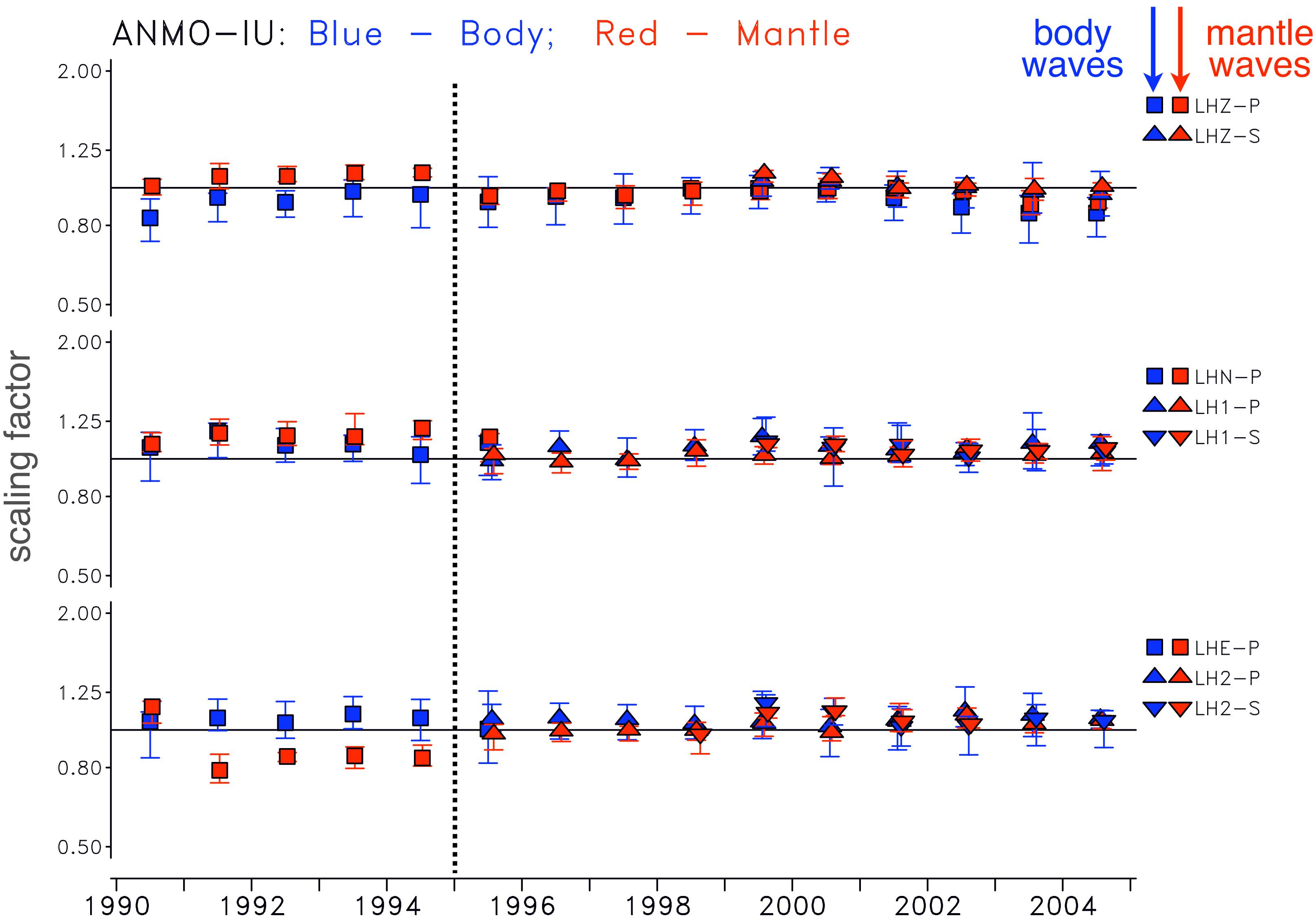

(Ekström, Dalton, and Nettles, SRL, 2006)

Scaling factors at PAB-IU, 1992-2004

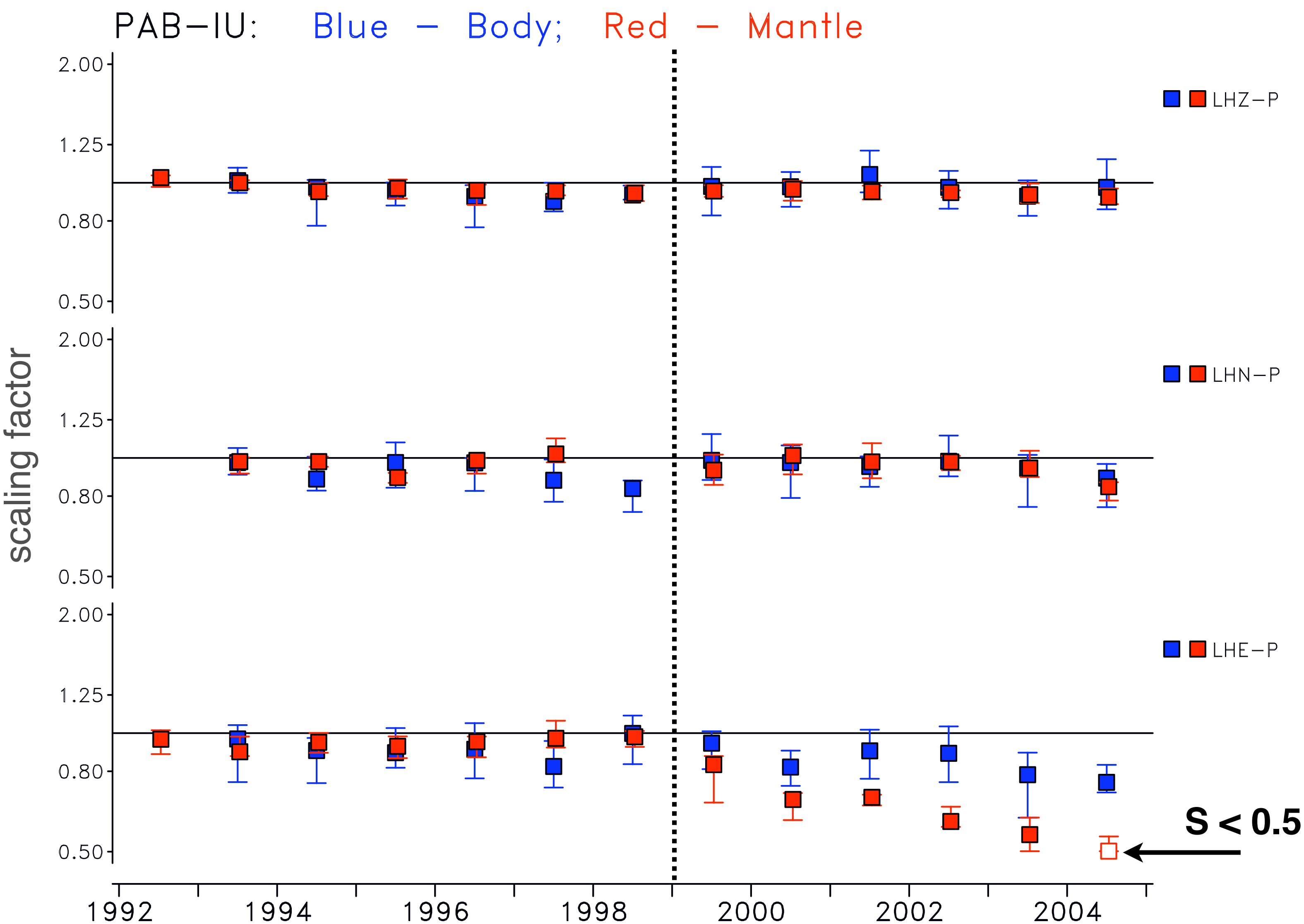

(Ekström, Dalton, and Nettles, SRL, 2006)

Scaling factors at LVZ-II, 1993-2004

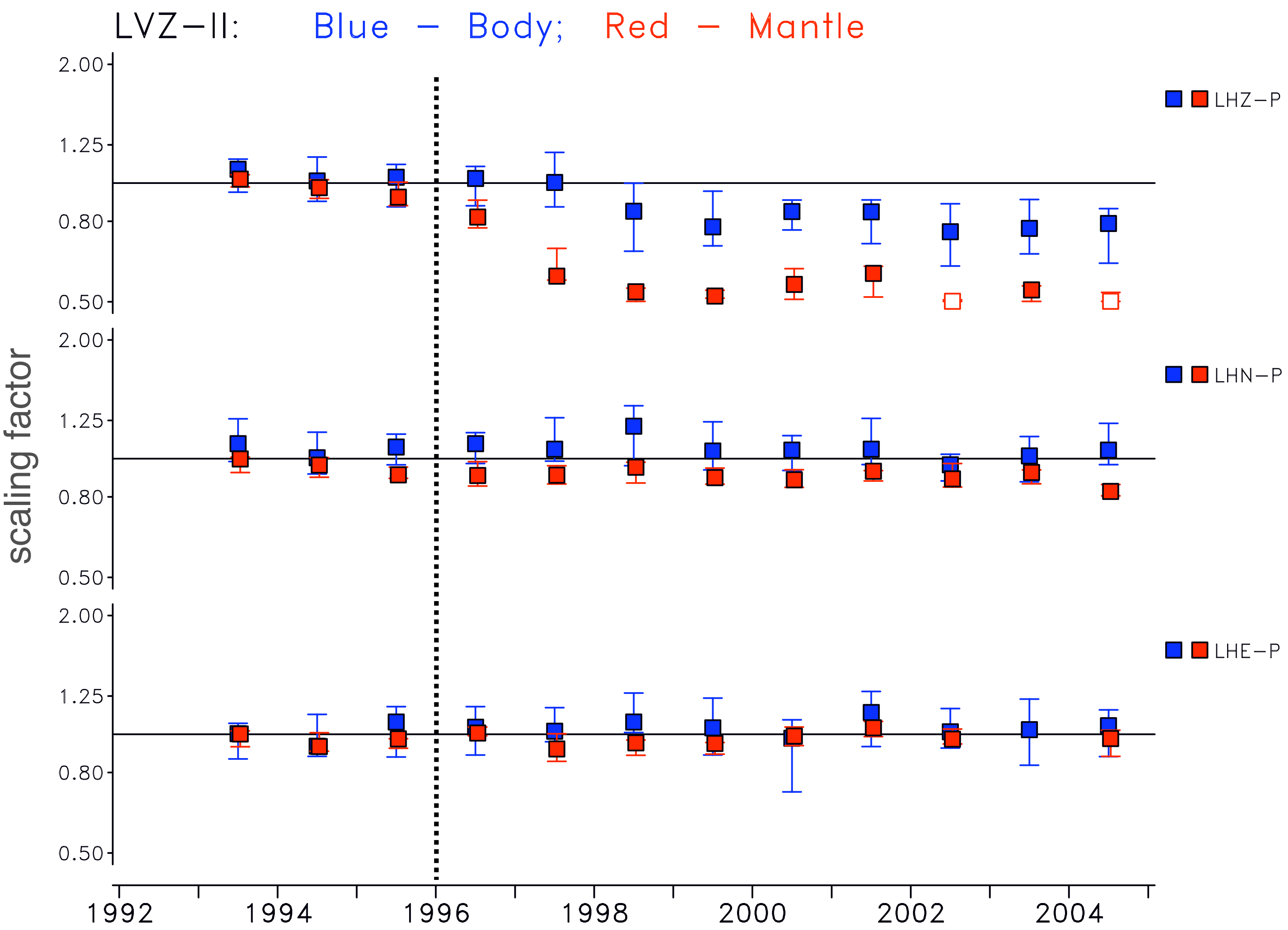

(Ekström, Dalton, and Nettles, SRL, 2006)

Scaling factors at CMB-BK, 1990-2004

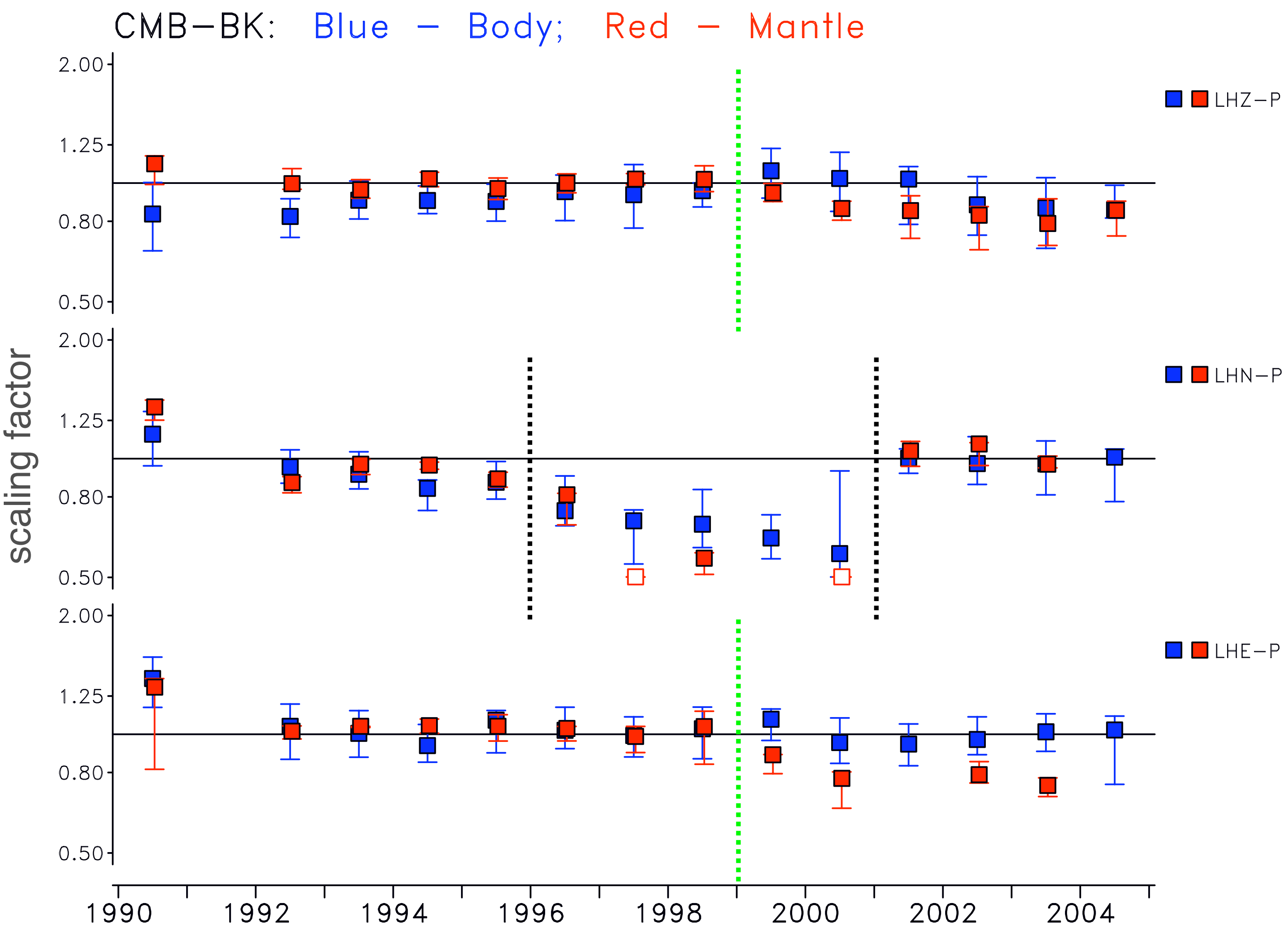

(Ekström, Dalton, and Nettles, SRL, 2006)

Scaling factors at PEL-G, 1996-2002

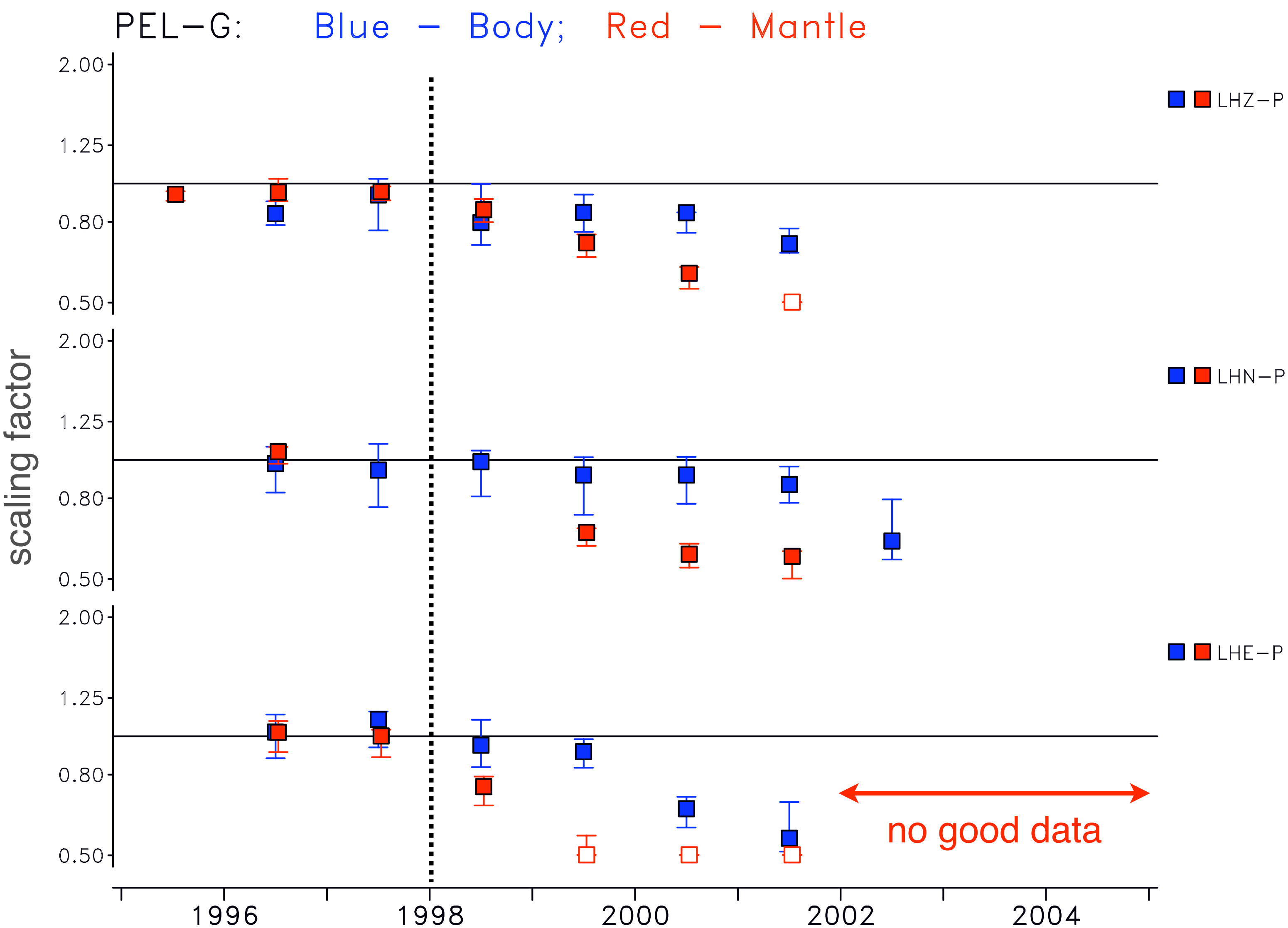

(Ekström, Dalton, and Nettles, SRL, 2006)

Scaling factors at SSE-IC, 1996-2004

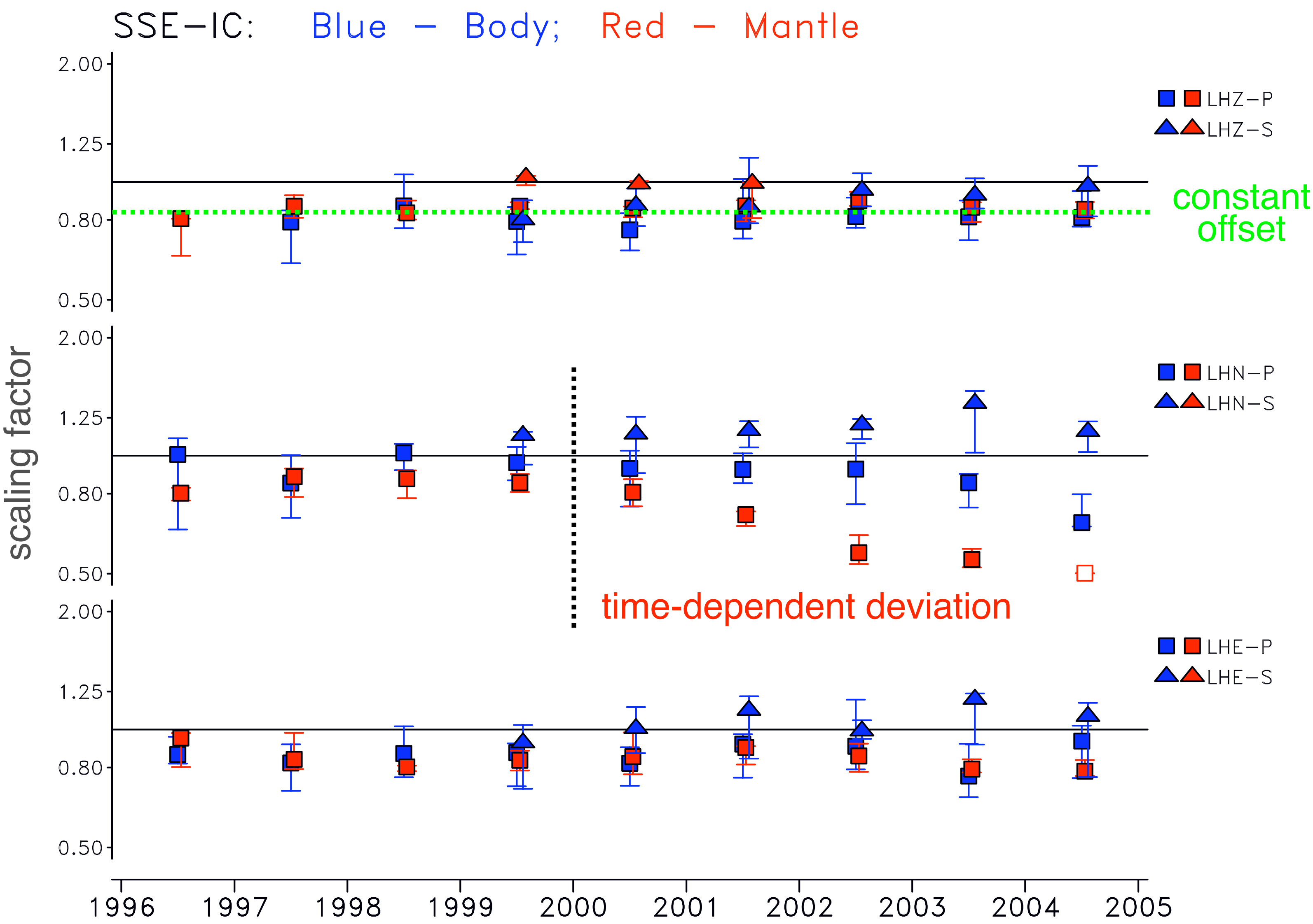

(Ekström, Dalton, and Nettles, SRL, 2006)

Most stations are well behaved

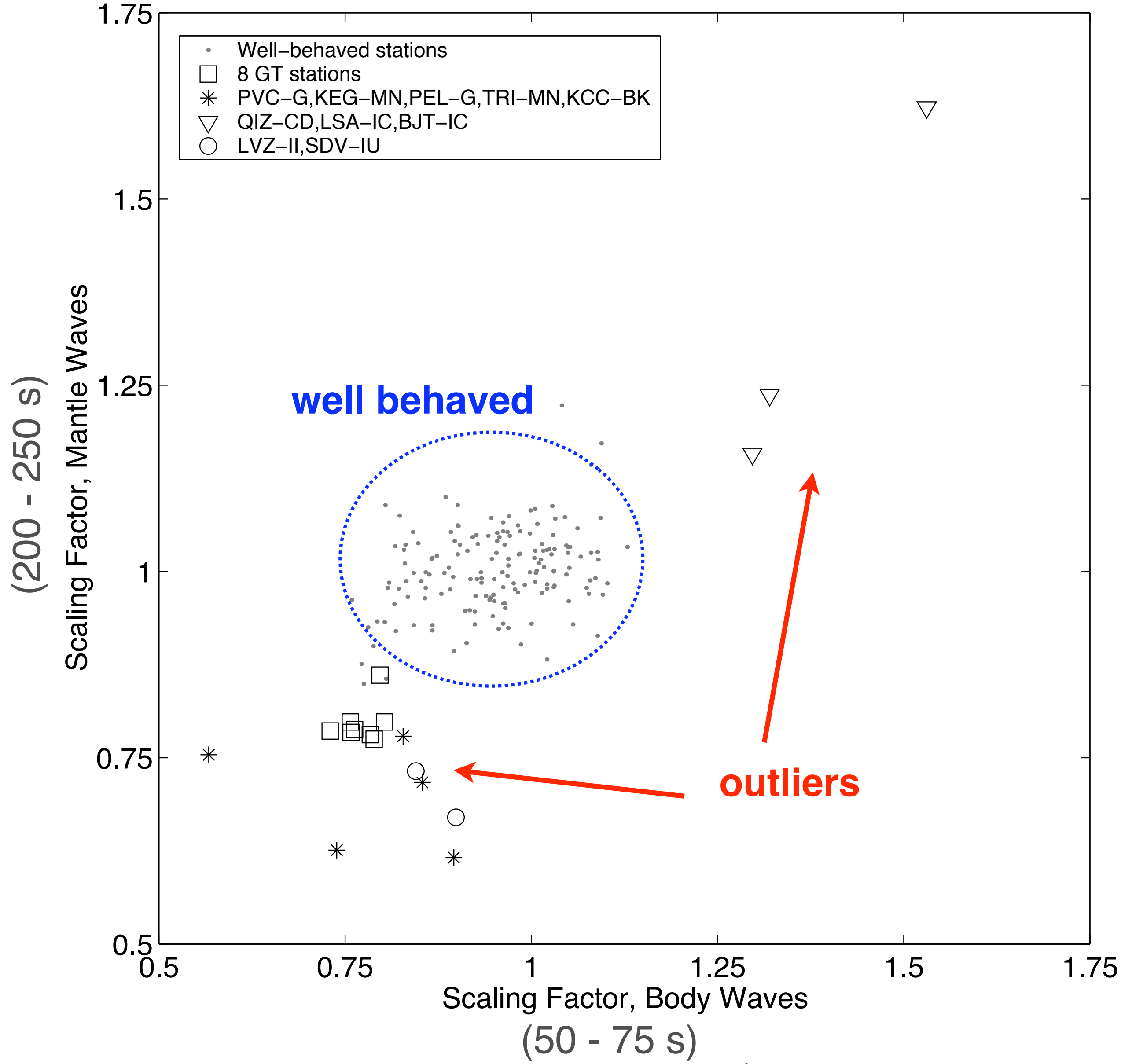

(Ekström, Dalton, and Nettles, SRL, 2006)

Stations for which a time- and frequency-dependent change in response is observed

Station	Network	Component	Start[a]	End[b]	Comment
ABKT	II	LHZ	1995	1997	
BJT	IC	LHZ	1999	2004	
BRVK	II	LHZ	2001	2004	
CMB	BK	LHE	1996	2000	Seismometer replaced in 2000
HRV	IU	LHE	1996	2004	
HRV	IU	LHN	1990	2004	
KCC	BK	LHZ	1999	2004	
KCC	BK	LHN	2000	2004	
KCC	BK	LHE	2002	2004	
KEG	MN	LHZ	1995	1998	No scaling data after 1998
KIP	IU	LHZ	2004	2004	Only one year with anomalous scaling
LVZ	II	LHZ	1995	2004	
MA2	IU	LHE	1998	2004	
PAB	IU	LHE	1999	2004	
PEL	G	LHZ	1999	2001	No scaling data after 2001
PEL	G	LHN	1999	2003	No scaling data after 2003
PEL	G	LHE	1998	2001	No scaling data after 2001
PET	IU	LHN	2002	2004	
SAO	BK	LHZ	2001	2004	
SSE	IC	LHN	2000	2004	
SSB	G	LHZ	2002	2004	

[a] Year in which the change in response is first clearly observed

[b] Year in which the change is last observed (2004 is the most recent year analyzed)

(Ekström, Dalton, and Nettles, SRL, 2006)

Summary

- All results are available at: www.seismology.harvard.edu/~ekstrom/Projects/WQC/SCALING
- Most stations show no, or small, deviations from the reported response
- A few stations (e.g., GTSN) show constant offsets in gain of 10-20%
- *Approximately 15% of stations equipped with STS-1 seismometers show a time- and frequency-dependent deterioration of the true gain*

➡ Cause of problem?

- ▸ How to fix instruments?
- ▸ How to fix response information retroactively?

➡ Recommend regular instrument calibration

6. Finding interesting things in the noise

Seismographs record signals with frequencies between ~10 Hz to 1000 seconds.

Earthquakes are detected and located using high-frequency signals (around 1 Hz).

Are there short-lived geophysical phenomena that generate seismic waves at long periods but that are not detected at short periods?

Kermadec to Pasadena, $\Delta = 85^{o}$

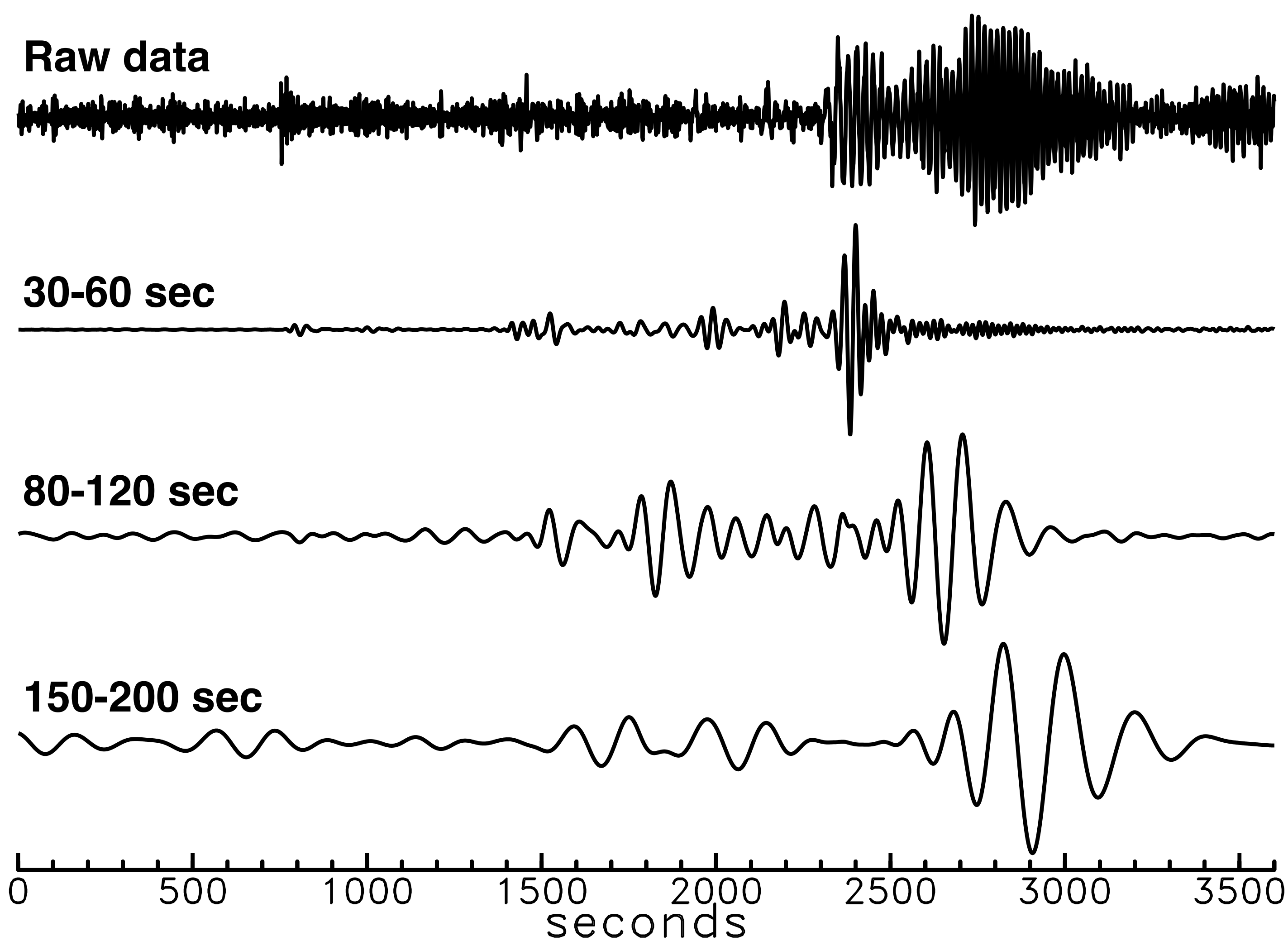

Surface-wave dispersion

Seismic surface waves are dispersive, $c = c(\omega)$, where $\omega = \frac{2\pi}{T}$ and T is the period of the waves.

Travel time τ is therefore dependent on frequency, $\tau(\omega)$.

Propagation phase $\Phi(\omega) = \omega \cdot \tau(\omega) = \frac{\tau(\omega) \cdot 2\pi}{T}$.

For the propagation phase from point (θ_A, φ_A) to point (θ_B, φ_B) we write,

$$\Phi(\omega) = \int_A^B \frac{\omega}{c(\theta, \varphi; \omega)} ds$$

with velocity depending on position, $c(\theta, \varphi)$.

GLOBAL SEISMOGRAPHIC NETWORK

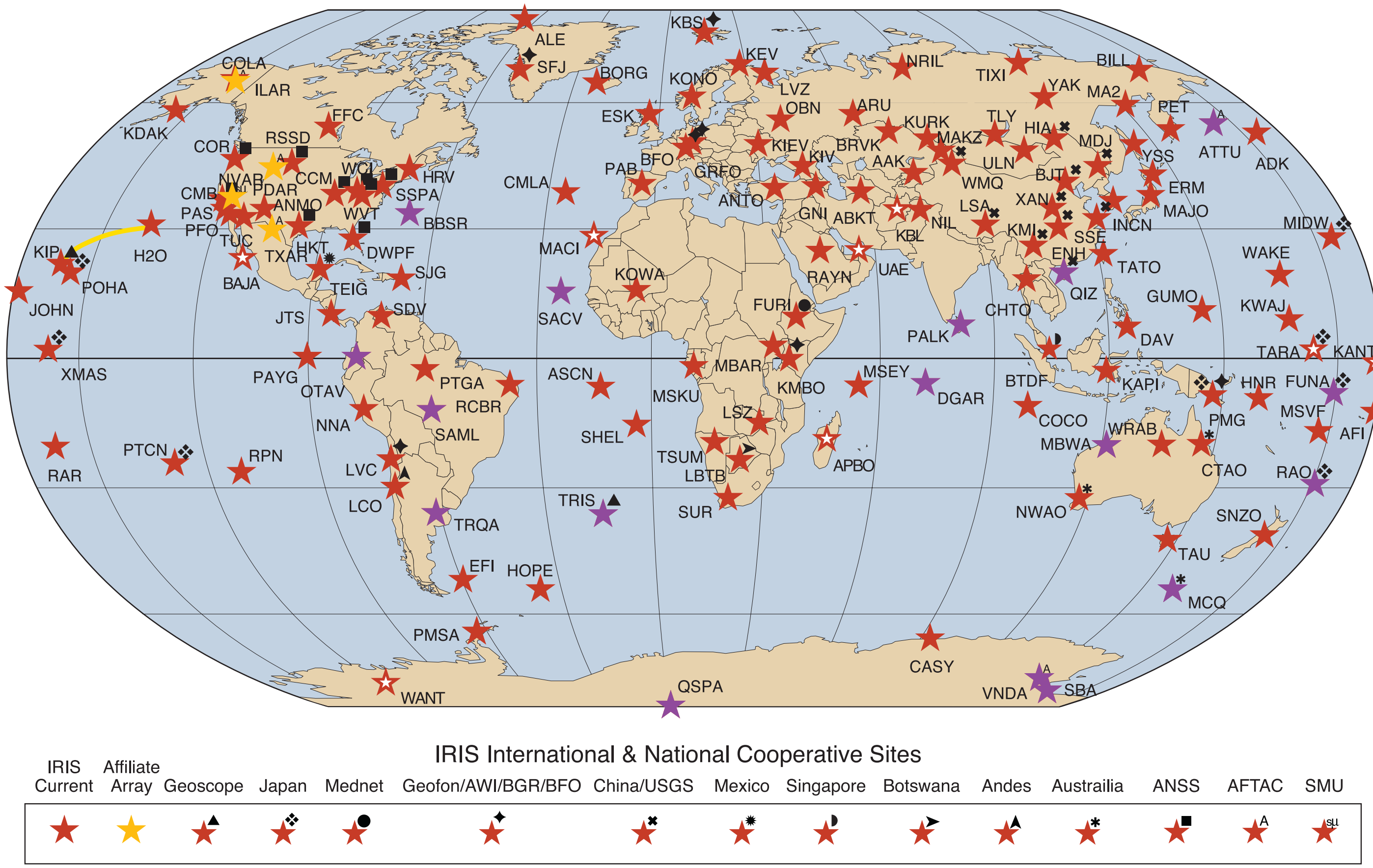

Current GSN station coverage of Earth is shown as of August 2005. Sites added in the past five years are noted in purple (stations) and orange (arrays). Sites planned to be completed are noted with white stars. Cooperative sites are indicated by symbols on the upper right "shoulder" of the stars.

1. Collect seismograms from the GSN

2. Low-pass filter, 35-250 s period

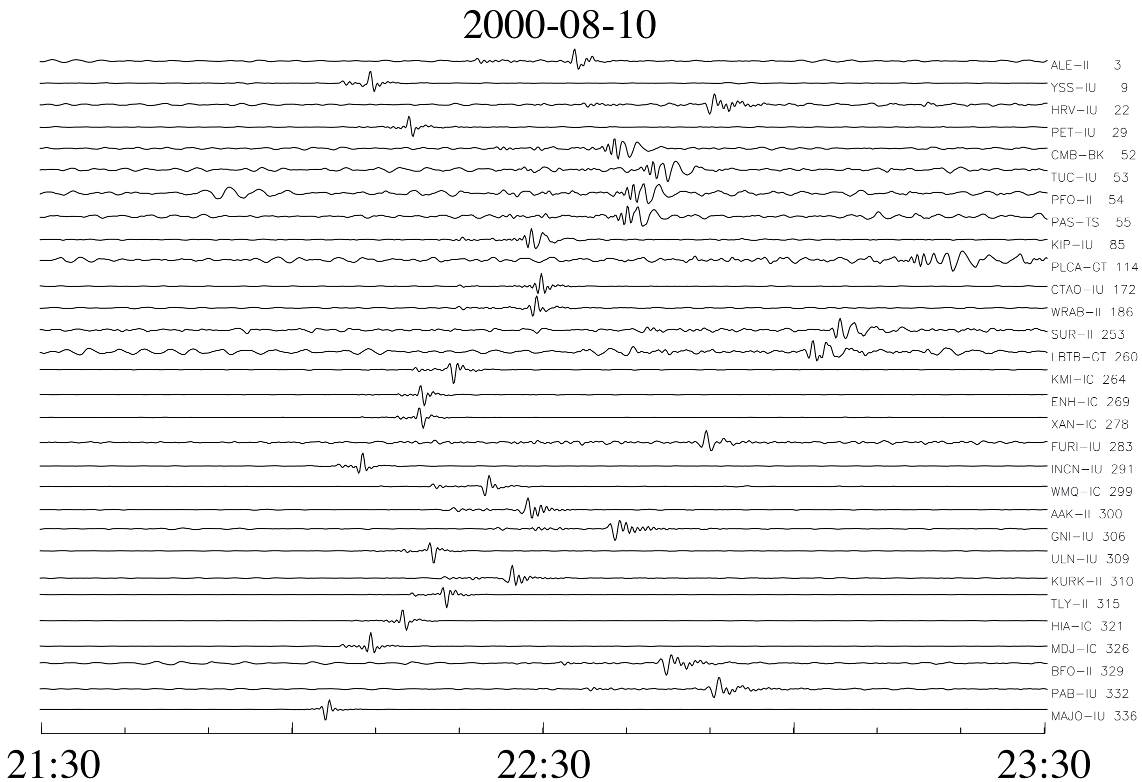

3. Select a target location

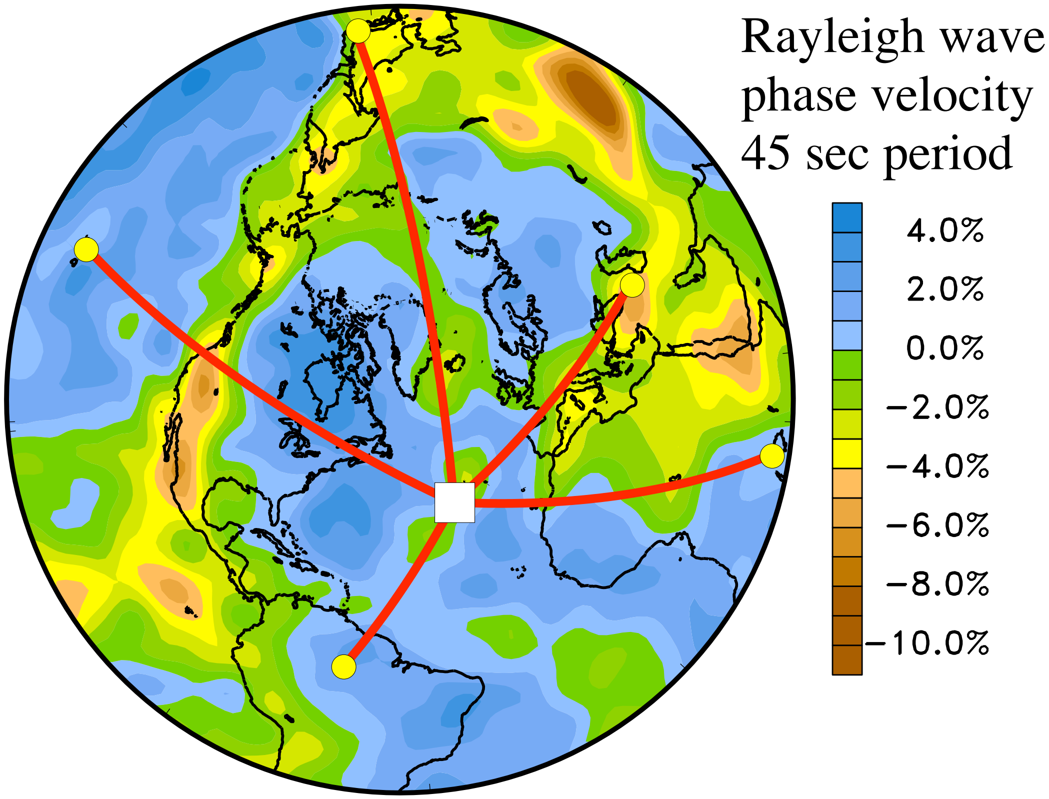

4. Calculate dispersion curves to all stations

5. Deconvolve propagation effects from all seismograms

6. Calculate envelope function

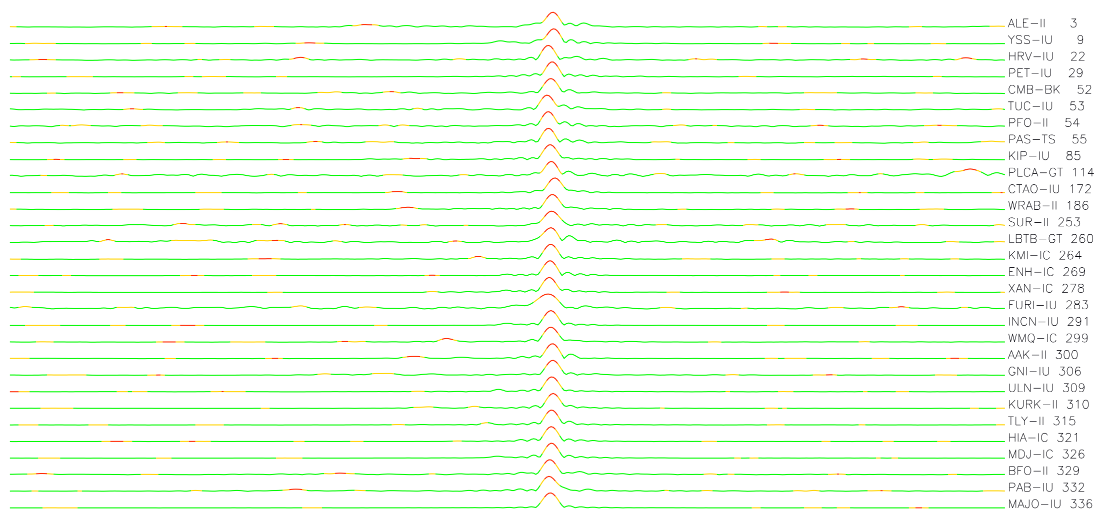

7. Stack

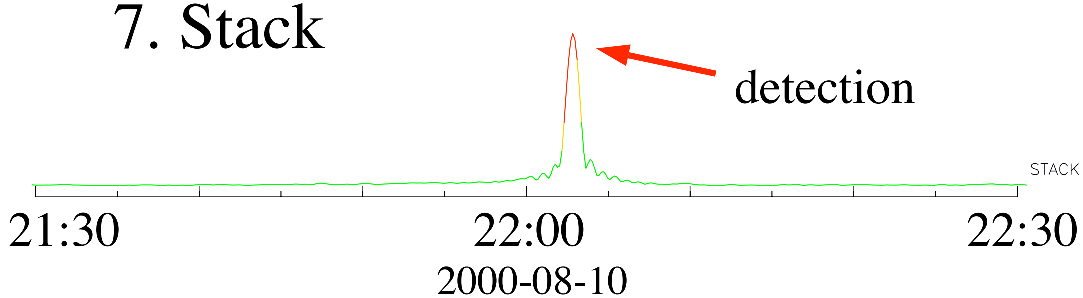

24,412 detected seismic events
1993-2003

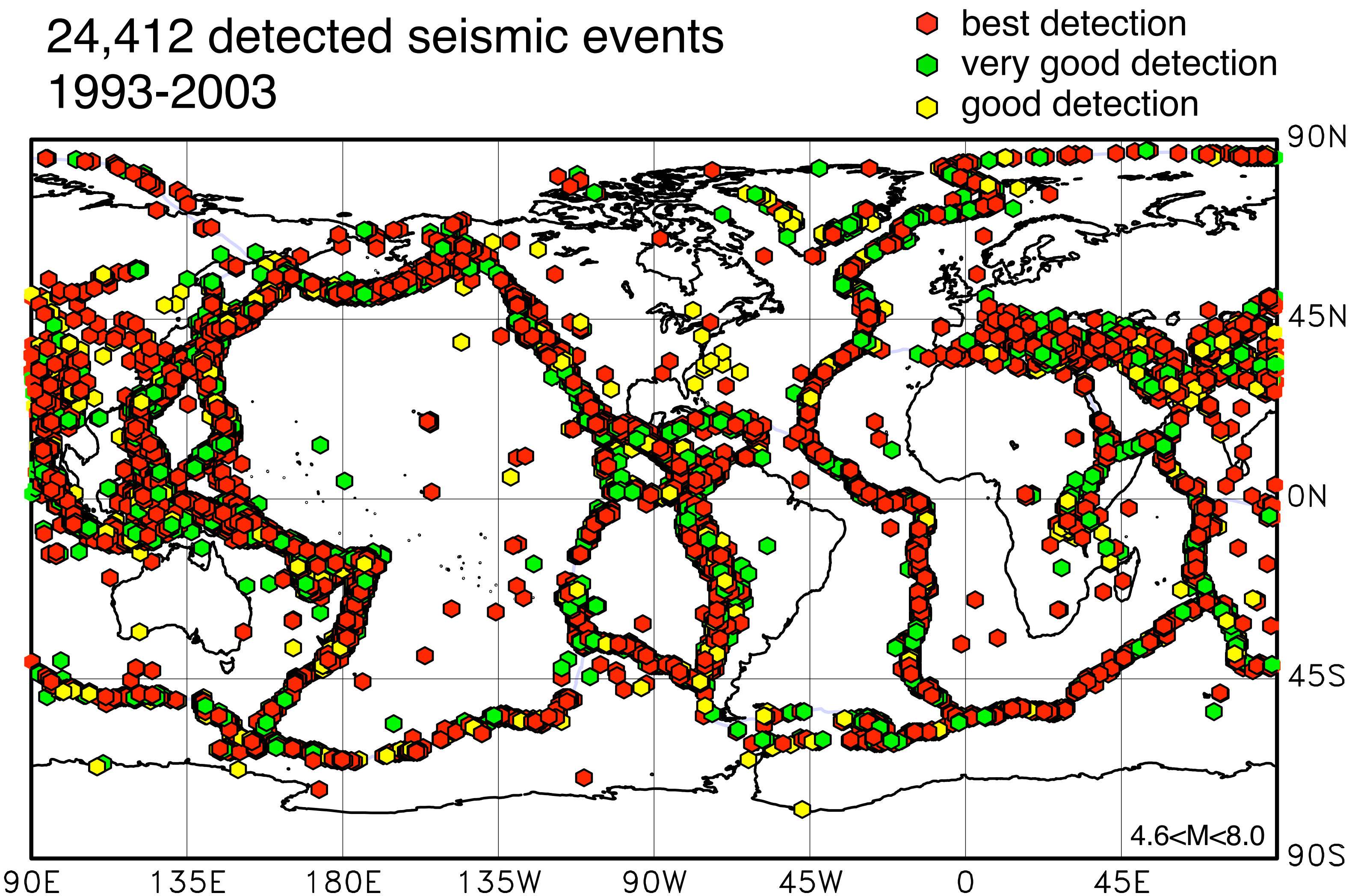

(Ekström, BSSA, 2006)

New earthquakes - not in other catalogs

1860 new seismic events
1993-2003

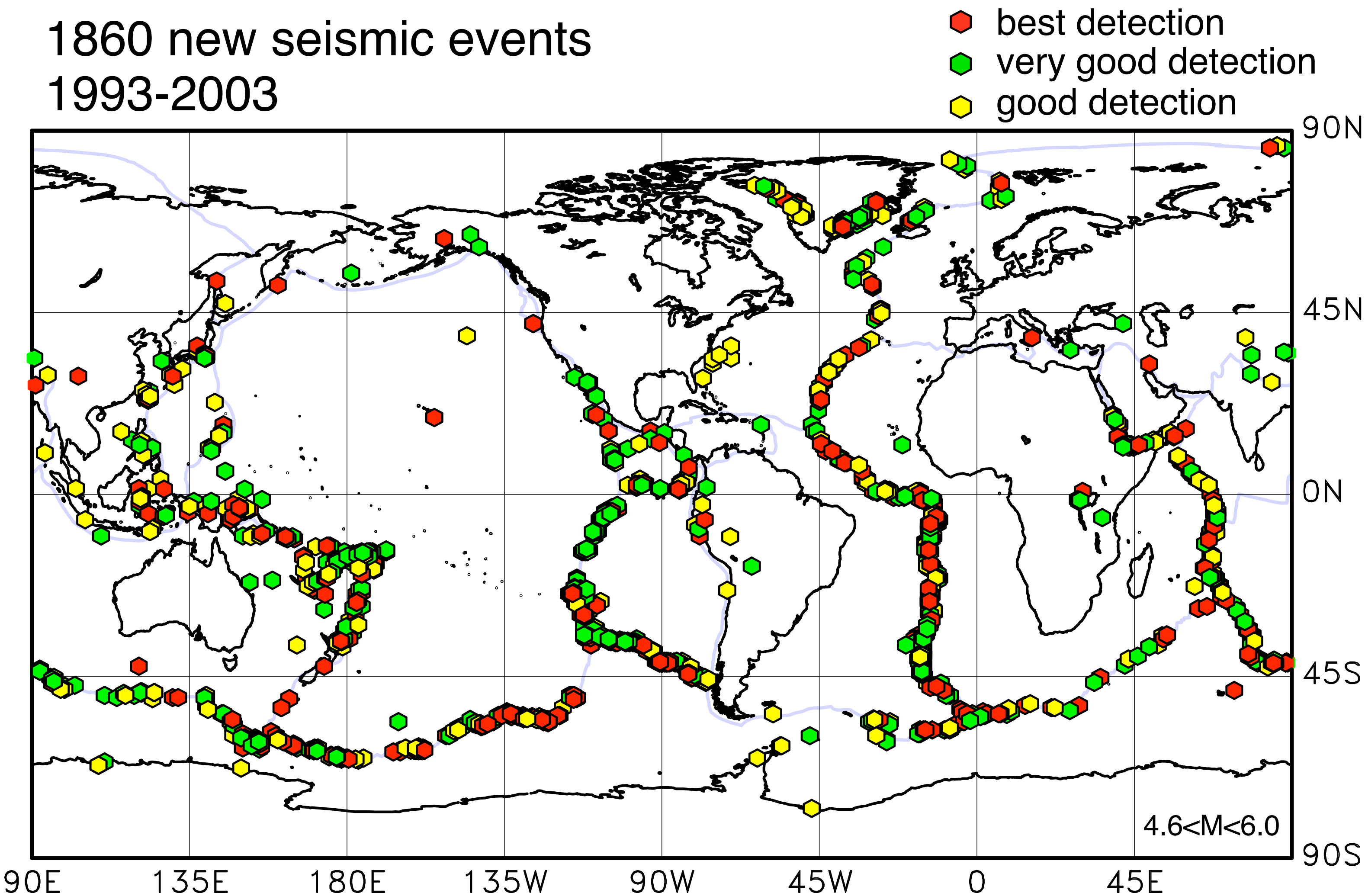

(Ekström, BSSA, 2006)

1999 Alaska Range earthquake detection

Approximate location of mystery event

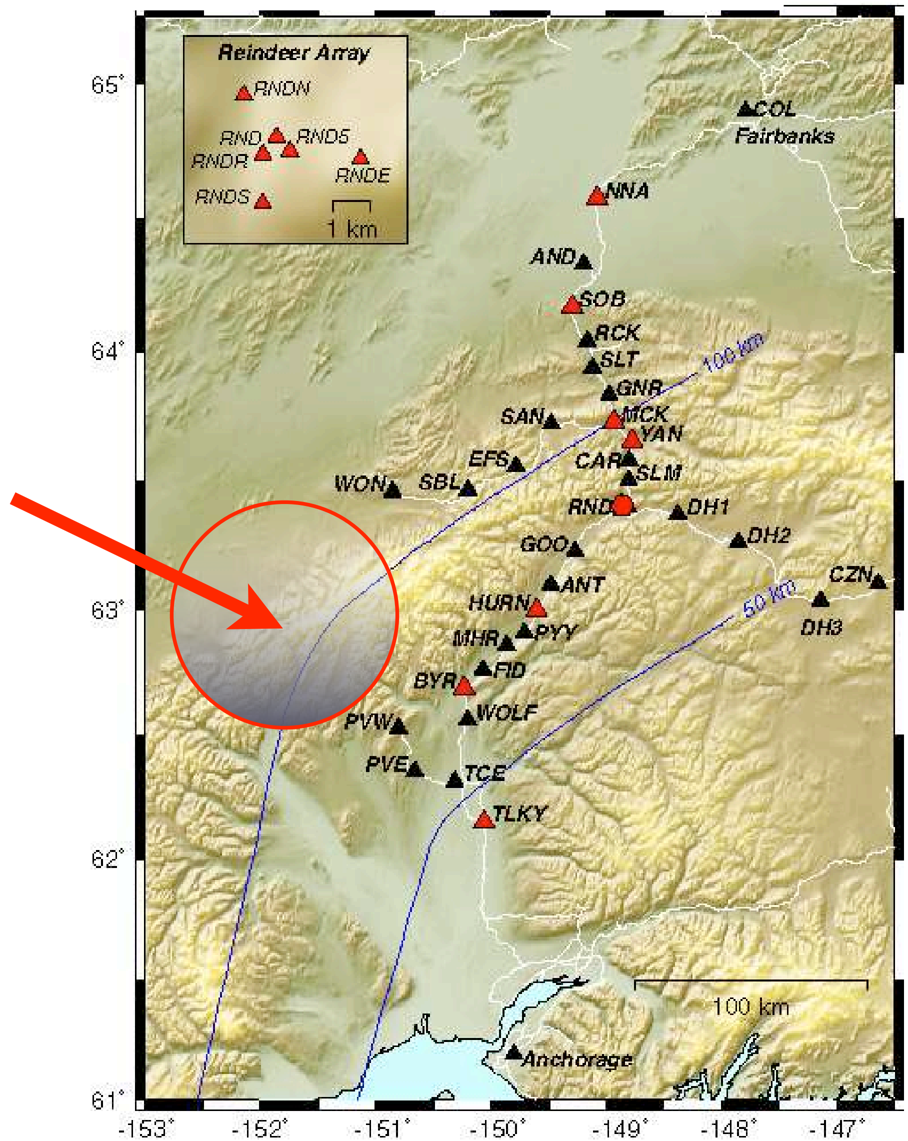

Comparison of seismograms

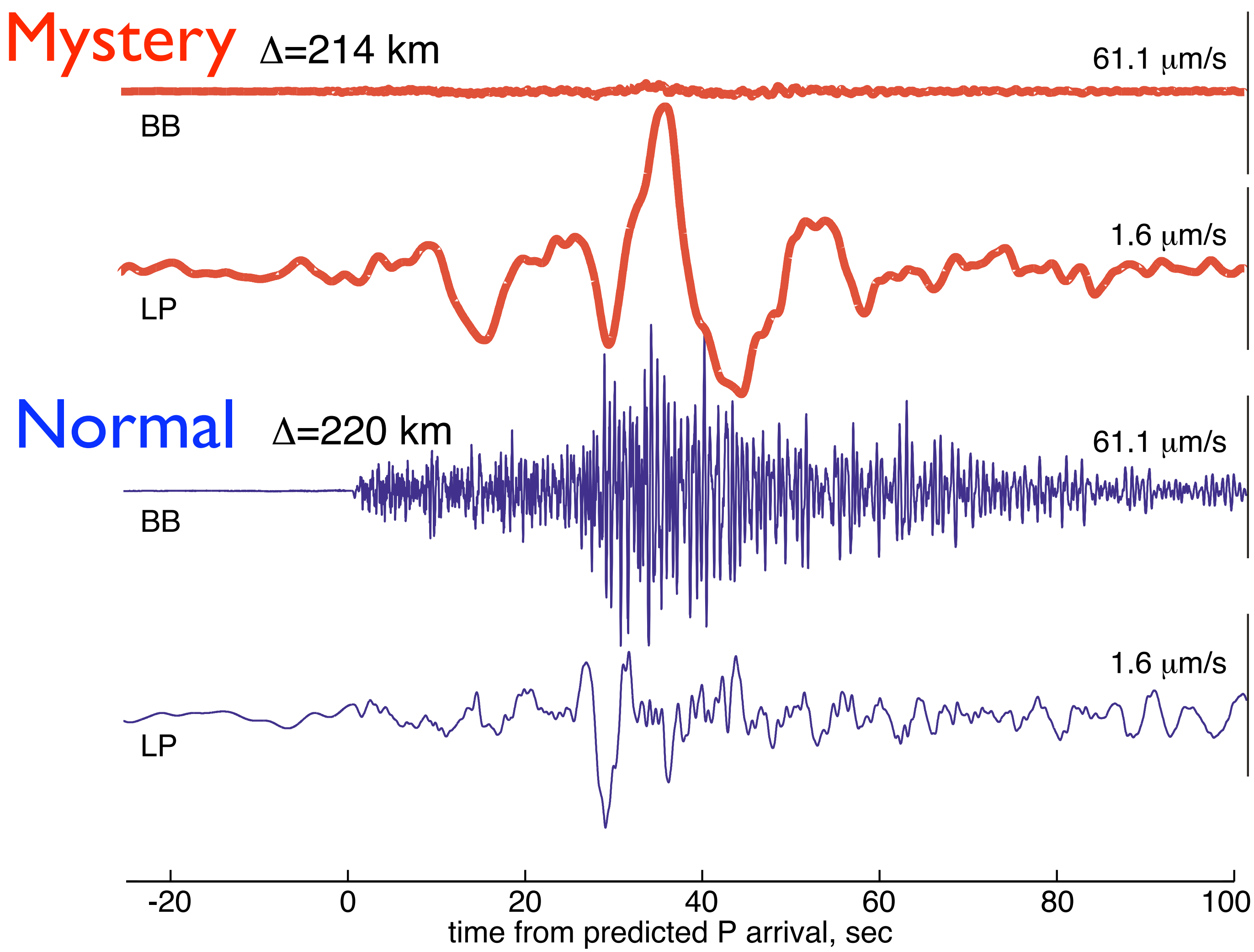

(Ekström, Nettles, and Abers, Science, 2003)

Faulting force model

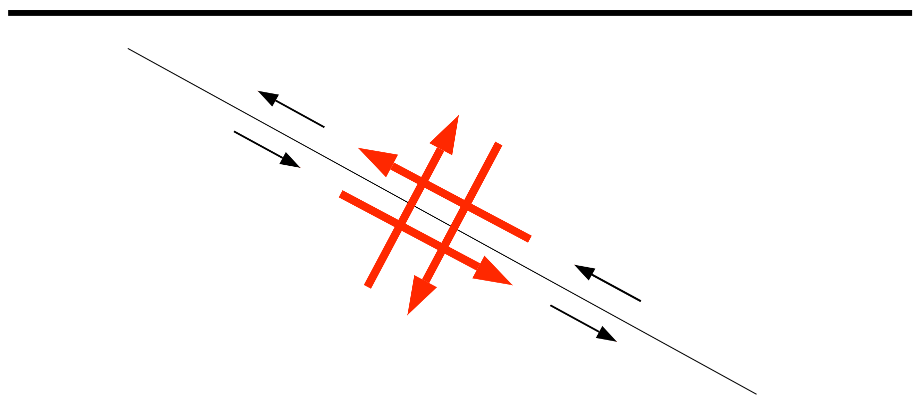

Landslide force model

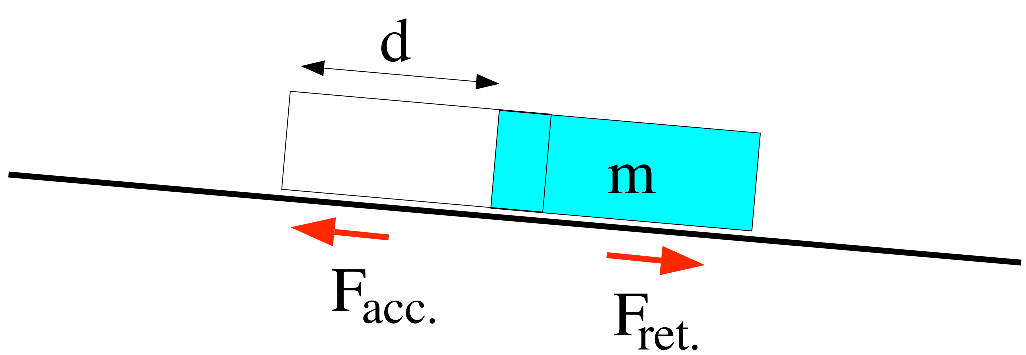

New earthquakes - not in other catalogs

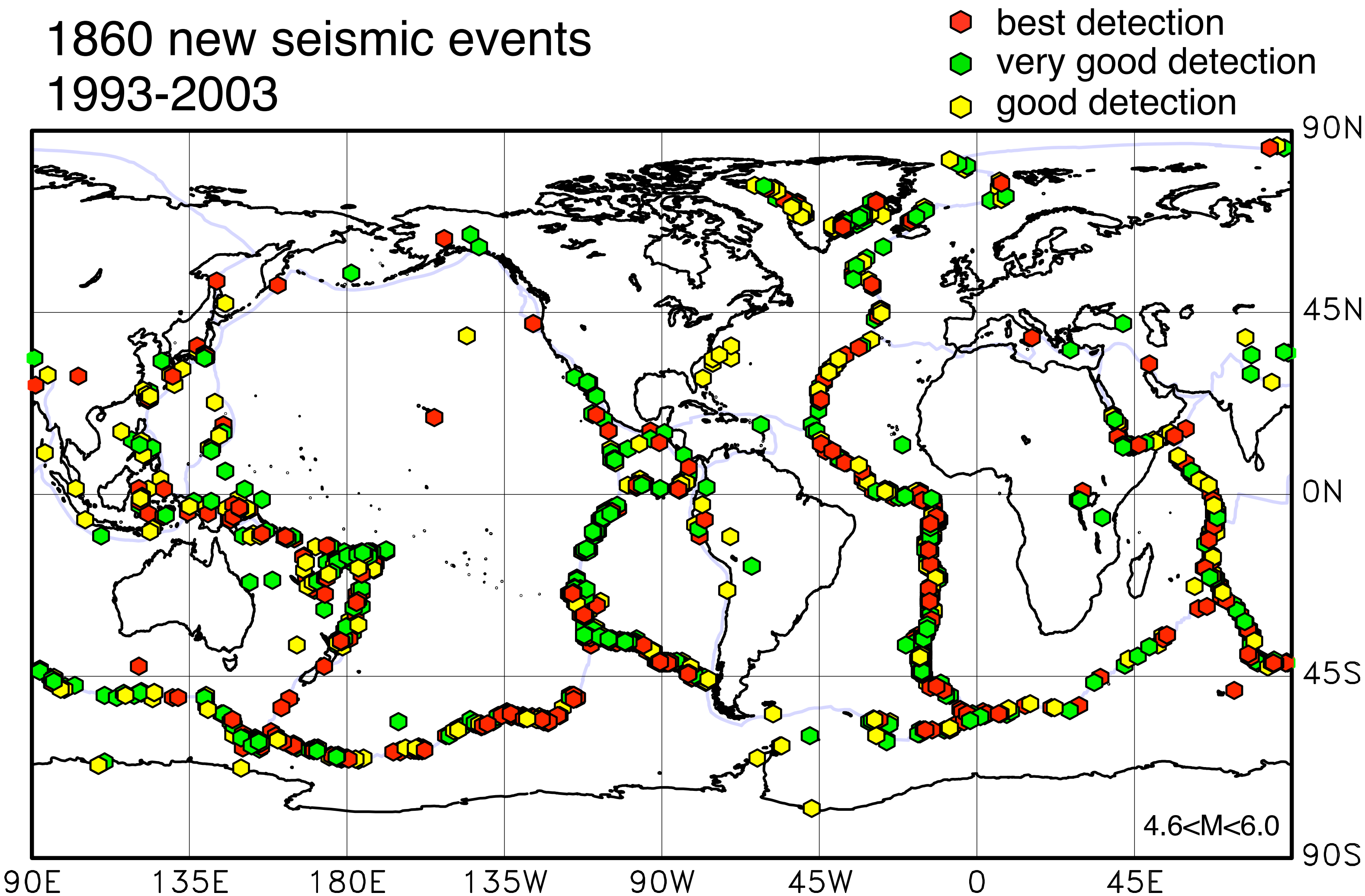

(Ekström, BSSA, 2006)

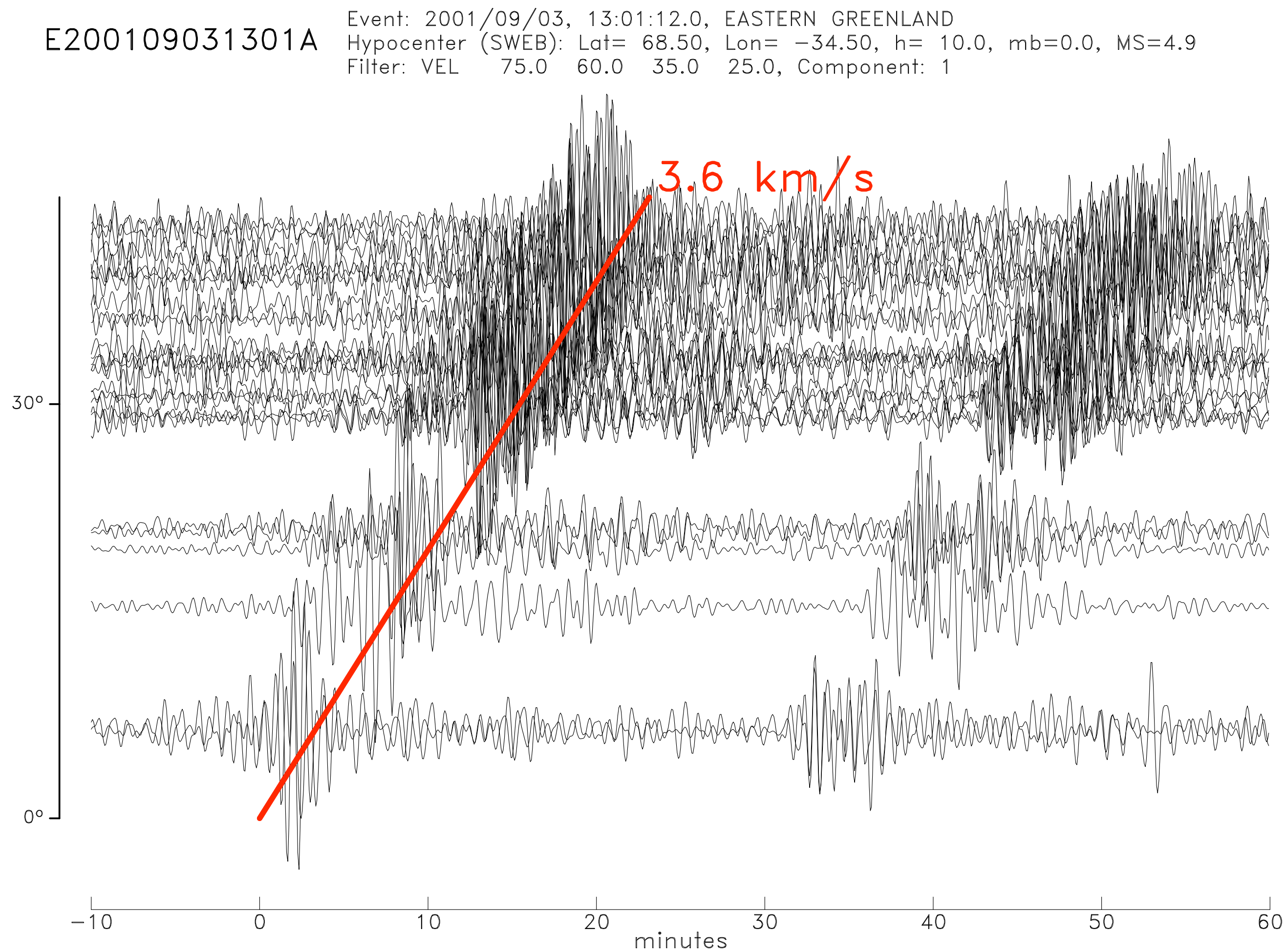
E200109031301A
Event: 2001/09/03, 13:01:12.0, EASTERN GREENLAND
Hypocenter (SWEB): Lat= 68.50, Lon= −34.50, h= 10.0, mb=0.0, MS=4.9
Filter: VEL 75.0 60.0 35.0 25.0, Component: 1
3.6 km/s
30°
0°
−10
0
10
20
30
40
50
60
minutes

136 glacial earthquakes

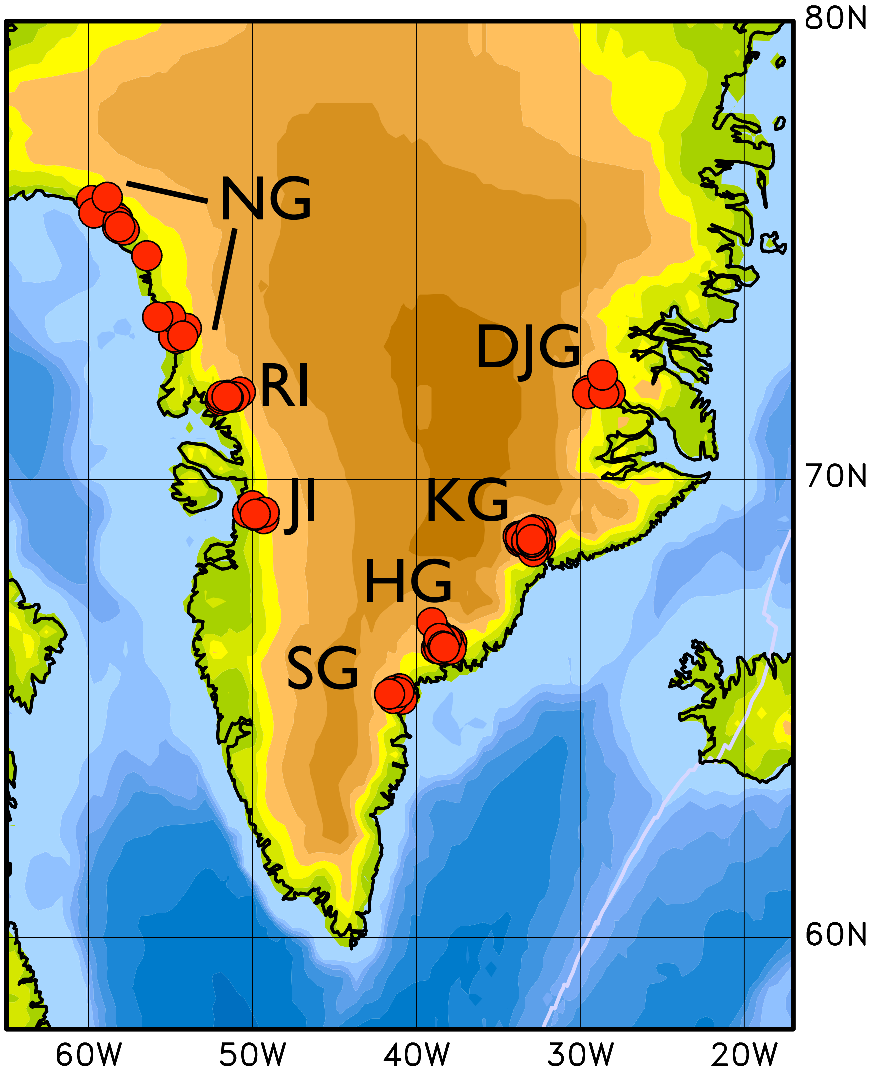

(Ekström, Nettles, and Tsai, Science, 2006)

Balance velocities of the ice

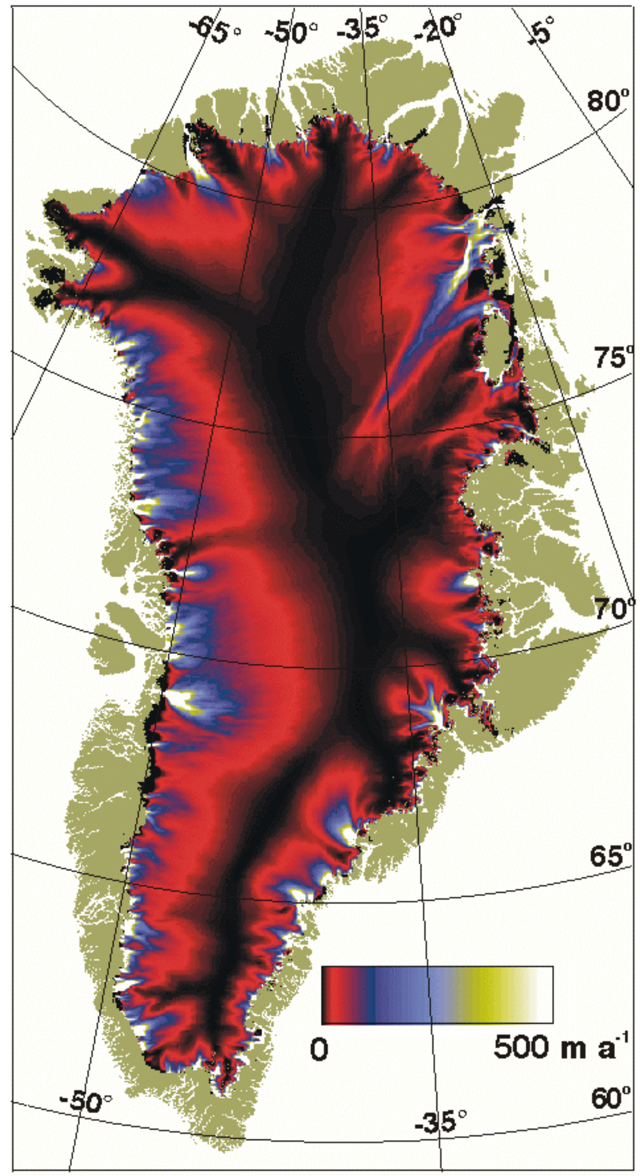

Bamber et al. (2002)

Seasonality of glacial earthquakes (1993-2004)

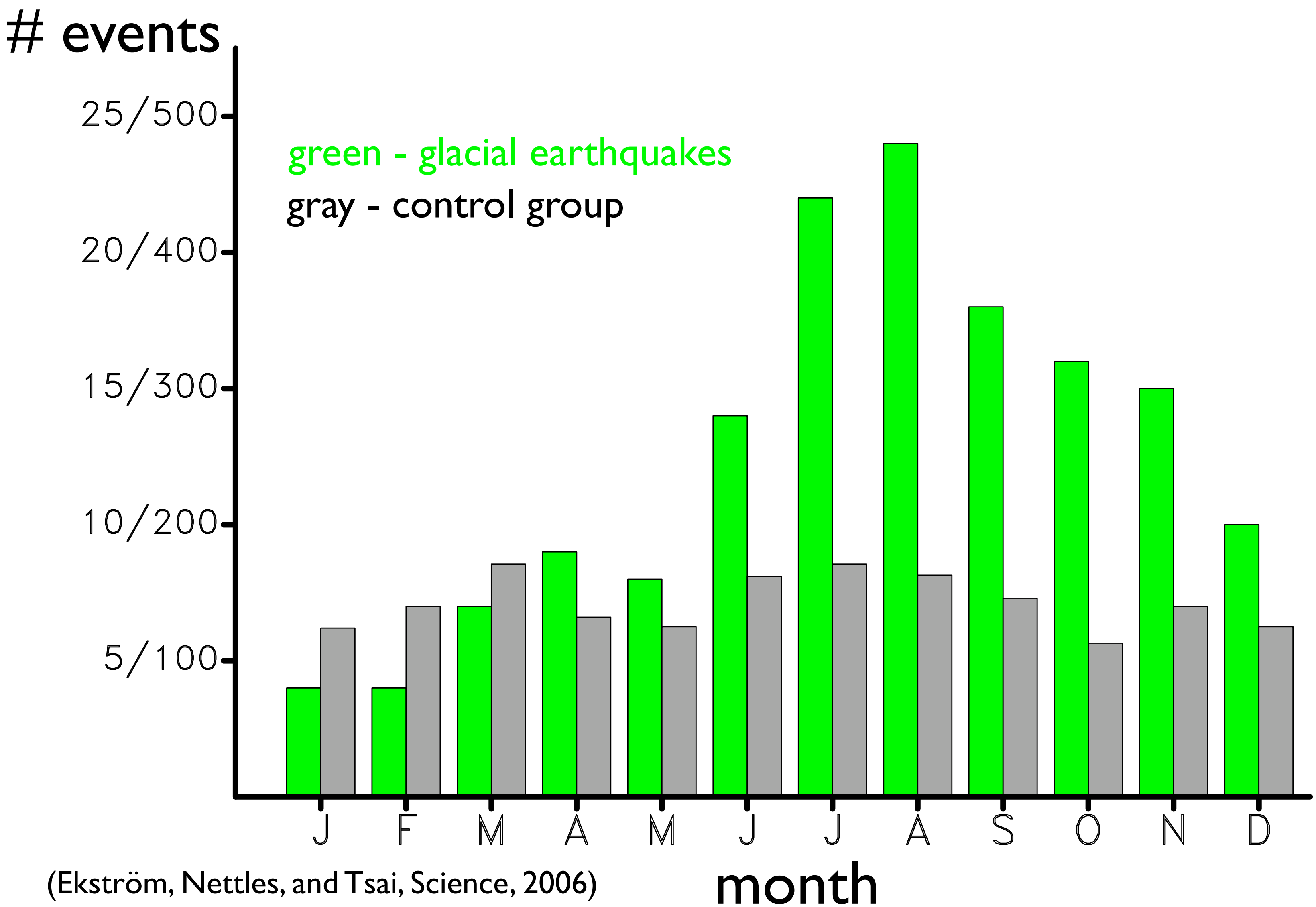

(Ekström, Nettles, and Tsai, Science, 2006)

Mechanism of melt water lubrication of glacial base

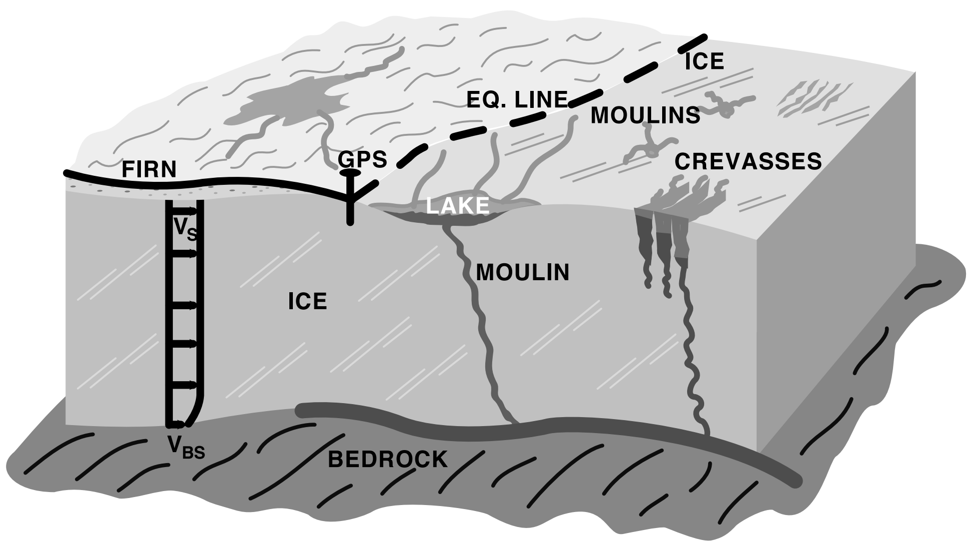

Fig. 2. Schematic of glaciological features in the equilibrium and ablation zones, including surface lakes, inflow channels, crevasses, and moulins. Ice flow for basal ice at the pressure melting point is partly from basal sliding and partly from shear deformation, which is mostly in a near-basal boundary layer.

from Zwally et al., Science, 2002

Increasing frequency of Greenland glacial earthquakes

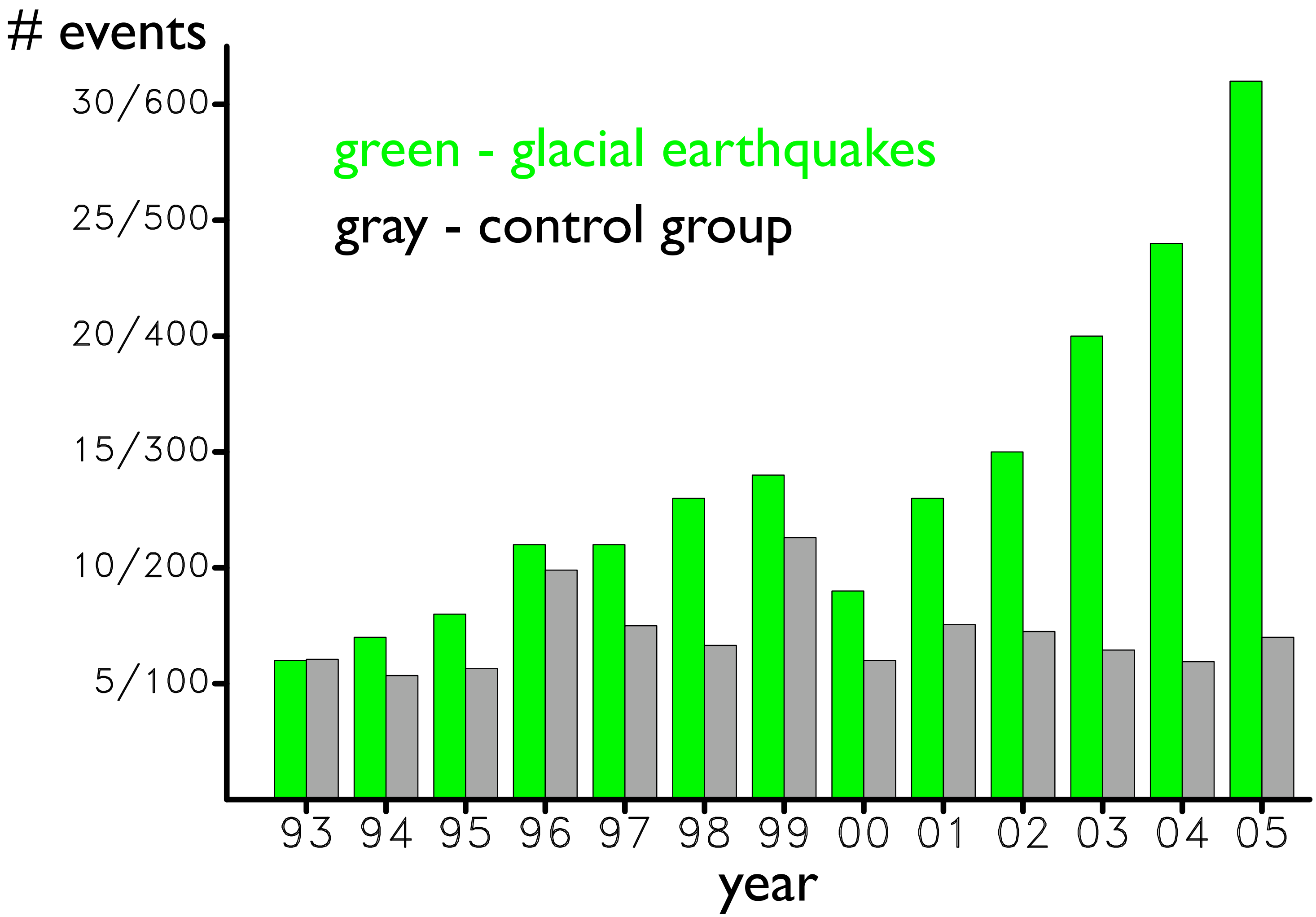

(Ekström, Nettles, and Tsai, Science, 2006)

Helheim Glacier, Eastern Greenland

Higher Speed

2000 2004

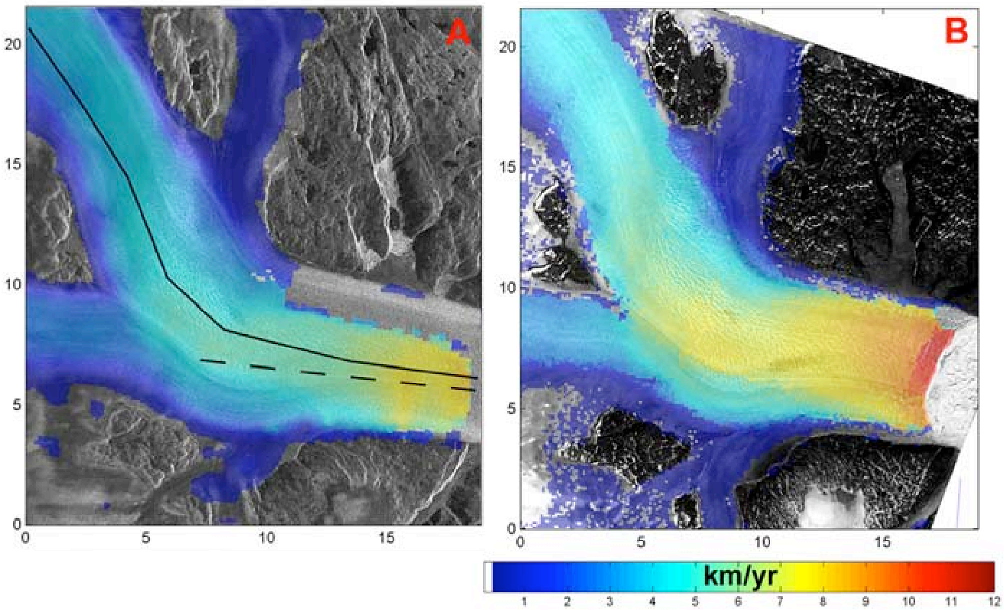

Retreat

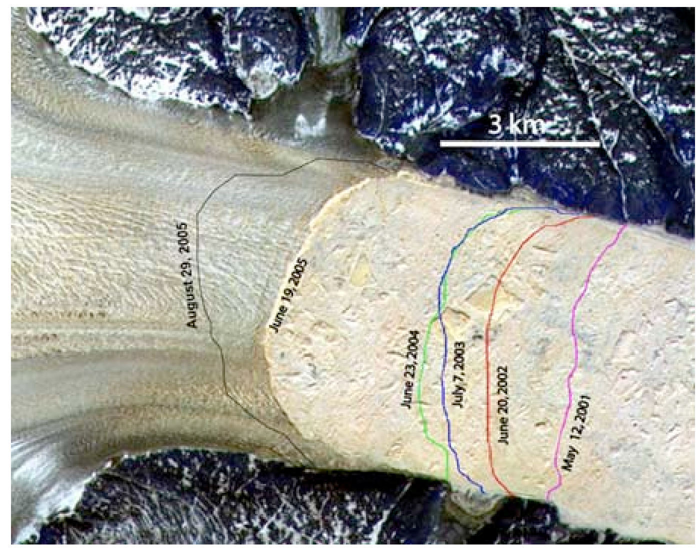

Howat et al., 2005; Hamilton & Stearns, 2005